Signal transducer and activator of transcription 1 (*STAT1*) gain-of-function mutations and disseminated coccidioidomycosis and histoplasmosis

Elizabeth P. Sampaio, MD, PhD,[a,b] Amy P. Hsu, BA,[a] Joseph Pechacek, BA,[a] Hannelore I. Bax, MD,[a,c] Dalton L. Dias, BA,[a] Michelle L. Paulson, MD,[d] Prabha Chandrasekaran, PhD,[a] Lindsey B. Rosen, BS,[a] Daniel S. Carvalho, PhD,[a,b] Li Ding, MD,[a] Donald C. Vinh, MD,[e] Sarah K. Browne, MD,[a] Shrimati Datta, PhD,[f] Joshua D. Milner, MD,[f] Douglas B. Kuhns, PhD,[g] Debra A. Long Priel, BS,[g] Mohammed A. Sadat, MD,[h] Michael Shiloh, MD, PhD,[i] Brendan De Marco, MD,[i] Michael Alvares, MD,[j] Jason W. Gillman, MD,[i] Vivek Ramarathnam, MD,[i] Maite de la Morena, MD,[j] Liliana Bezrodnik, MD,[k] Ileana Moreira, MD,[k] Gulbu Uzel, MD,[a] Daniel Johnson, MD,[l] Christine Spalding, RN,[a] Christa S. Zerbe, MD,[a] Henry Wiley, MD,[m] David E. Greenberg, MD,[i] Susan E. Hoover, MD, PhD,[n] Sergio D. Rosenzweig, MD, PhD,[h,o] John N. Galgiani, MD,[n] and Steven M. Holland, MD[a] *Bethesda and Frederick, Md, Rio de Janeiro, Brazil, Rotterdam, The Netherlands, Montreal, Quebec, Canada, Dallas, Tex, Buenos Aires, Argentina, Chicago, Ill, and Tucson, Ariz*

Background: Impaired signaling in the IFN-γ/IL-12 pathway causes susceptibility to severe disseminated infections with mycobacteria and dimorphic yeasts. Dominant gain-of-function mutations in signal transducer and activator of transcription 1 (*STAT1*) have been associated with chronic mucocutaneous candidiasis.
Objective: We sought to identify the molecular defect in patients with disseminated dimorphic yeast infections.
Methods: PBMCs, EBV-transformed B cells, and transfected U3A cell lines were studied for IFN-γ/IL-12 pathway function. STAT1 was sequenced in probands and available relatives. Interferon-induced STAT1 phosphorylation, transcriptional responses, protein-protein interactions, target gene activation, and function were investigated.
Results: We identified 5 patients with disseminated *Coccidioides immitis* or *Histoplasma capsulatum* with heterozygous missense mutations in the *STAT1* coiled-coil or DNA-binding domains. These are dominant gain-of-function mutations causing enhanced STAT1 phosphorylation, delayed dephosphorylation, enhanced DNA binding and transactivation, and enhanced interaction with protein inhibitor of activated STAT1. The mutations caused enhanced IFN-γ–induced gene expression, but we found impaired responses to IFN-γ restimulation.
Conclusion: Gain-of-function mutations in *STAT1* predispose to invasive, severe, disseminated dimorphic yeast infections, likely through aberrant regulation of IFN-γ–mediated inflammation. (J Allergy Clin Immunol 2013;■■■:■■■-■■■.)

Key words: *Signal transducer and activator of transcription 1, IFN-γ, progressive multifocal leukoencephalopathy,* Histoplasma capsulatum*,* Coccidioides immitis*, thrush*

The IFN-γ/IL-12 signaling pathway controls extrapulmonary infections with bacteria, such as nontuberculous mycobacteria, BCG, *Mycobacterium tuberculosis*, and *Salmonella* species,[1,2] as well as the dimorphic fungi *Histoplasma capsulatum*,[3] *Paracoccidioides brasiliensis*,[4] and *Coccidioides immitis*.[5,6] Stimulation of IFN-γ and IFN-α receptors leads to phosphorylation of signal transducer and activator of transcription 1 (STAT1), which homodimerizes and heterodimerizes before translocating to the nucleus, where interferon-induced genes are activated.[7] Complete recessive mutations in *STAT1* cause susceptibility to viral, mycobacterial, and bacterial infections, whereas heterozygous inhibitory *STAT1* mutations cause mild disseminated BCG or nontuberculous mycobacterial infections.[8-10] Recently, dominant gain-of-function mutations in *STAT1* were described as causing chronic mucocutaneous candidiasis (CMC), impaired STAT1 dephosphorylation, and diminished numbers of IL-17–producing T cells.[11,12]

The regulation of STAT1 activity includes the suppressor of cytokine signaling and protein inhibitor of activated STAT (PIAS)

From [a]the Immunopathogenesis Section, Laboratory of Clinical Infectious Diseases, [f]the Allergic Inflammation Unit, Laboratory of Allergic Diseases, [h]the Infectious Diseases Susceptibility Unit, Laboratory of Host Defenses, and [o]the Primary Immunodeficiency Clinic, National Institute of Allergy and Infectious Diseases (NIAID), National Institutes of Health (NIH), Bethesda; [b]the Leprosy Laboratory, Oswaldo Cruz Institute, FIOCRUZ, Rio de Janeiro; [c]the Department of Internal Medicine and Department of Medical Microbiology and Infectious Diseases, Erasmus Medical Center, Rotterdam; [d]the Clinical Research Directorate/CMRP and [g]the Clinical Services Program, SAIC-Frederick, NCI-Frederick, Frederick; [e]the Division of Infectious Diseases, McGill University Health Centre, Montreal; [i]the Division of Infectious Diseases and [j]the Division of Allergy and Immunology, University of Texas Southwestern Medical Center, Dallas; [k]the Immunology Unit, Pediatric Hospital R. Gutierrez, Buenos Aires; [l]Comer Children's Hospital, University of Chicago; [m]the Clinical Trials Branch, National Eye Institute, NIH, Bethesda; and [n]Valley Fever Center for Excellence, University of Arizona College of Medicine, Tucson.

Supported by the Division of Intramural Research, National Institute of Allergy and Infectious Diseases, National Institutes of Health, and funded in part with federal funds from the National Cancer Institute, National Institutes of Health, under contract no. HHSN261200800001E. The content of this publication does not necessarily reflect the views or policies of the Department of Health and Human Services nor does mention of trade names, commercial products, or organizations imply endorsement by the US Government.

Disclosure of potential conflict of interest: D. C. Vinh has received research support from the Canadian Institutes of Health Research Post-doctoral Fellowship, CSL Behring Canada, and Astellas Canada; has consultant arrangements with CSL Behring Canada and Pfizer Canada; and has received payment for lectures from CSL Behring Canada and Sunovion/Sepracor. D. B. Kuhns and D. A. Long Priel have received grants from the National Cancer Institute/National Institutes of Health. V. Ramarathnam is employed by Private Practice ID. S. D. Rosenzweig receives royalties from UpToDate. The rest of the authors declare that they have no relevant conflicts of interest.

Received for publication June 20, 2012; revised October 22, 2012; accepted for publication January 23, 2013.

Corresponding author: Steven M. Holland, MD, CRC B3-4141 MSC 1684, Bethesda, MD 20892-1684. E-mail: smh@nih.gov.

0091-6749
http://dx.doi.org/10.1016/j.jaci.2013.01.052

Abbreviations used

CMC:	Chronic mucocutaneous candidiasis
CSF:	Cerebrospinal fluid
CT:	Computed tomography
DMA:	Mono/dimethylarginine antibody
GAS:	Gamma-activated sequence
GFP:	Green fluorescent protein
ISRE:	Type I interferon response element
L-AmB:	Liposomal amphotericin B
MRI:	Magnetic resonance imaging
NIH:	National Institutes of Health
PIAS:	Protein inhibitor of activated STAT
PML:	Progressive multifocal leukoencephalopathy
pSTAT1:	Phosphorylated STAT1
SAMe:	S-adenosylmethionine
siRNA:	Small interfering RNA
STAT1:	Signal transducer and activator of transcription 1
WB:	Western blotting
WT:	Wild-type

families of proteins.[13,14] Posttranslational modifications of STATs (acetylation, methylation, SUMOylation, and ISG15ylation among others) also regulate their function and response. PIAS1 is thought to interfere with STAT1 DNA binding and to recruit other transcriptional coregulators. PIAS proteins have also been shown to have E3 ligase activity and to promote protein SUMOylation.[15]

We identified 5 patients with disseminated dimorphic fungal infections who had mutations in *STAT1*: 2 patients had disseminated refractory coccidioidomycosis beginning in childhood or adolescence without CMC, and 3 patients had disseminated histoplasmosis and CMC, including 1 patient who also had progressive multifocal leukoencephalopathy (PML). These are gain-of-function mutations that ultimately lead to delayed dephosphorylation of STAT1, lower STAT1 methylation, enhanced STAT1/PIAS1 association, and an impaired response to IFN-γ restimulation.

METHODS

Patients and blood samples

All samples were collected under approved National Institutes of Health (NIH) protocols; all patients or their parents provided written informed consent. Healthy volunteer blood samples were obtained under approved protocols through the Department of Transfusion Medicine, NIH.

Cell lines

EBV-transformed B-cell lines derived from patients and healthy donors were maintained in RPMI 1640 with 20% FCS, 2 mmol/L L-glutamine, 100 U/mL penicillin, and 100 μg/mL streptomycin at 37°C in a humidified 5% CO_2 incubator. STAT1-deficient U3A cells (generously provided by G. Stark, Cleveland Clinic, Cleveland, Ohio) were maintained in complete Dulbecco modified Eagle medium (see the Methods section in this article's Online Repository at www.jacionline.org).

STAT1 sequencing

Genomic DNA (PureGene Gentra DNA isolation kit; Qiagen, Hilden, Germany) and total RNA (STAT-60 RNA isolation kit; Tel-Test, Friendswood, Tex) were extracted from EBV-transformed B-cell lines or polymorphonuclear leukocytes. Primers spanning exons and flanking splice sites of human genomic *STAT1* and full-length cDNA were designed with Primer Select (Lasergene; DNASTAR, Madison, Wis). Genomic amplification was performed with Platinum PCR Supermix High Fidelity (Invitrogen, Carlsbad, Calif). Samples were treated with ExoSAP (Affymetrix, Santa Clara, Calif), and 1 μL of the resulting product was used in sequencing reactions with Big Dye Terminators v3.1 (Applied Biosystems, Foster City, Calif), purified with Performa DTR short-well plate kit (Edge BioSystems, Gaithersburg, Md), and run on an Applied Biosystems 3730XL sequencer. Alignment was to the consensus sequence NM_007315.3 using Sequencer software (Gene Codes, Ann Arbor, Mich).

Constructs

Mutated STAT1 sequences or green fluorescent protein (GFP)–tagged constructs were created with a STAT1 expression vector (BioInnovatise, Rockville, Md). Wild-type (WT) and mutant STAT1 plasmids were isolated with the QIAprep Miniprep Kit (Qiagen), according to the manufacturer's recommendations, and all mutations were verified by means of sequencing. Transient transfection of U3A cells was done with the Nucleofactor Amaxa device (Lonza, Walkersville, Md), according to the manufacturer's recommendations.

Reporter gene assay

U3A cells were cotransfected with WT and/or mutant STAT1 expression constructs along with a plasmid containing tandem interferon-response elements (gamma-activated sequence [GAS] and type I interferon response element [ISRE]) driving a luciferase reporter gene (1 μg; Panomics, Fremont, Calif). A Renilla expression vector was cotransfected to measure transfection efficiency. Cells were stimulated with human IFN-γ or IFN-α2b at 1000 IU/mL for 6 hours. Luciferase activity was evaluated with a dual luciferase assay (Promega, Madison, Wis; see the Methods section in this article's Online Repository). Data are expressed as the fold increase in response to interferon over the WT unstimulated samples.

Evaluation of STAT1 activation

Phosphorylated STAT1 (pSTAT1) was assayed in U3A and EBV-B cells stimulated with IFN-γ (400 IU/mL) or IFN-α (1,000 IU/mL). For evaluation of dephosphorylation, pSTAT1 kinetics were assayed in cells stimulated with IFN-γ from 30 to 120 minutes. Cell lysates were recovered and analyzed by means of Western blotting (WB) and flow cytometry. For immunoprecipitation, cell lysates were incubated with anti-STAT1 antibody and protein G–Sepharose (Amersham Biosciences, Piscataway, NJ) overnight at 4°C, and immunoreactive proteins were resolved by means of WB.

Downregulation of PIAS1

High-purity small interfering RNA (siRNA) oligonucleotides that target PIAS1 and a control siRNA were obtained from Darmacon (Thermo Scientific, Lafayette, Colo). U3A cells were transiently transfected with the siRNA (ON-TARGET*plus* SMARTpool siRNA, 50 nmol/L) through eletroporation (Nucleofactor Amaxa), cotransfected with WT or mutant STAT1 constructs, and stimulated with IFN-γ (400 IU/mL).

Real-time PCR

Total RNA was extracted from cultured cells (PBMCs isolated from venous blood by means of density centrifugation and transfected U3A cells) with the RNeasy Mini Kit (Qiagen). For real-time PCR, 1 μg of total RNA was reverse transcribed (Invitrogen), and the resulting cDNA was amplified by means of PCR with the ABI 7500 Sequencer and TaqMan expression assays (Applied Biosystems). Glyceraldehyde-3-phosphate dehydrogenase was used as a normalization control. The data were analyzed with the $2^{-\Delta\Delta CT}$ method, and results were expressed as mean fold induction.

Statistical analysis

Results are reported as means ± SDs, unless otherwise stated. Differences between groups were assessed by using the Student *t* test (GraphPad Prism;

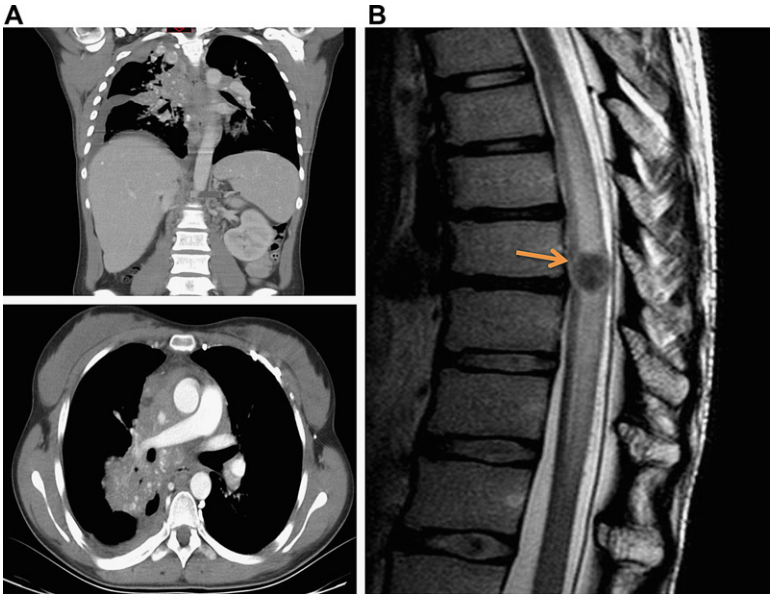

FIG 1. Patient 1. **A,** Extensive right upper lung, mediastinal, and pleural involvement with *C immitis*. **B,** MRI showing an intramedullary spinal cord lesion *(arrow)* with edema and cord compression.

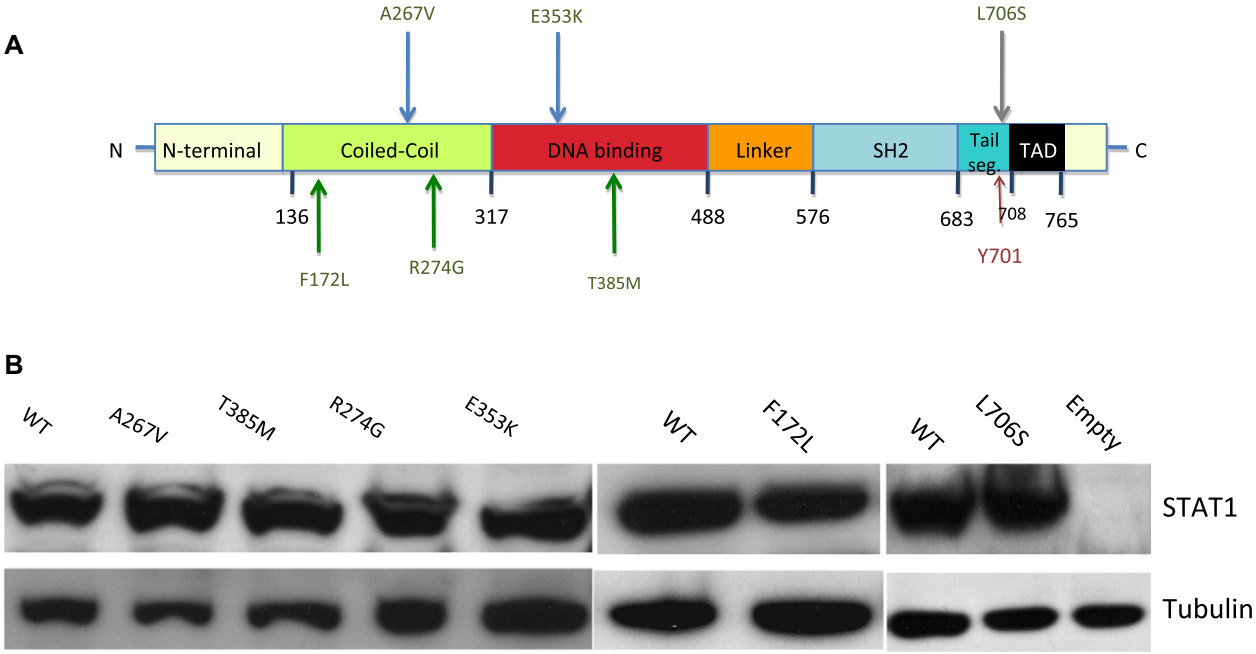

FIG 2. *STAT1* mutants. **A,** STAT1 coding region. *TAD,* Transactivation domain. Mutations were associated with *(blue arrows)* disseminated coccidioidomycosis and *(green arrows)* disseminated histoplasmosis. L706S was the dominant negative mutation. **B,** U3A cells transfected with STAT1 mutants, WT or empty vector, and WB with anti-STAT1 and anti-tubulin antibodies.

GraphPad Software, San Diego, Calif). The statistical significance level adopted was a *P* value of less than .05.

RESULTS

Patient 1 is a Hispanic female native of Arizona with no relevant previous or family history who presented at 14 years of age with extensive persistent tinea capitis and kerion caused by *Trichophyton tonsurans*. At age 17 years, she had prolonged cough, a painless right neck mass, fatigue, and weight loss. Computed tomography (CT) demonstrated multiple nodules throughout both lungs. CT confirmed diffuse progression with new osteomyelitis at vertebral bodies C6 through T5 and multiple lesions throughout the liver and spleen. She received liposomal amphotericin B (L-AmB) and voriconazole and then posaconazole. At age 20 years, a new *Coccidioides* species–induced skin lesion developed that was associated with anorexia and weight loss. Magnetic resonance imaging (MRI) demonstrated progressive

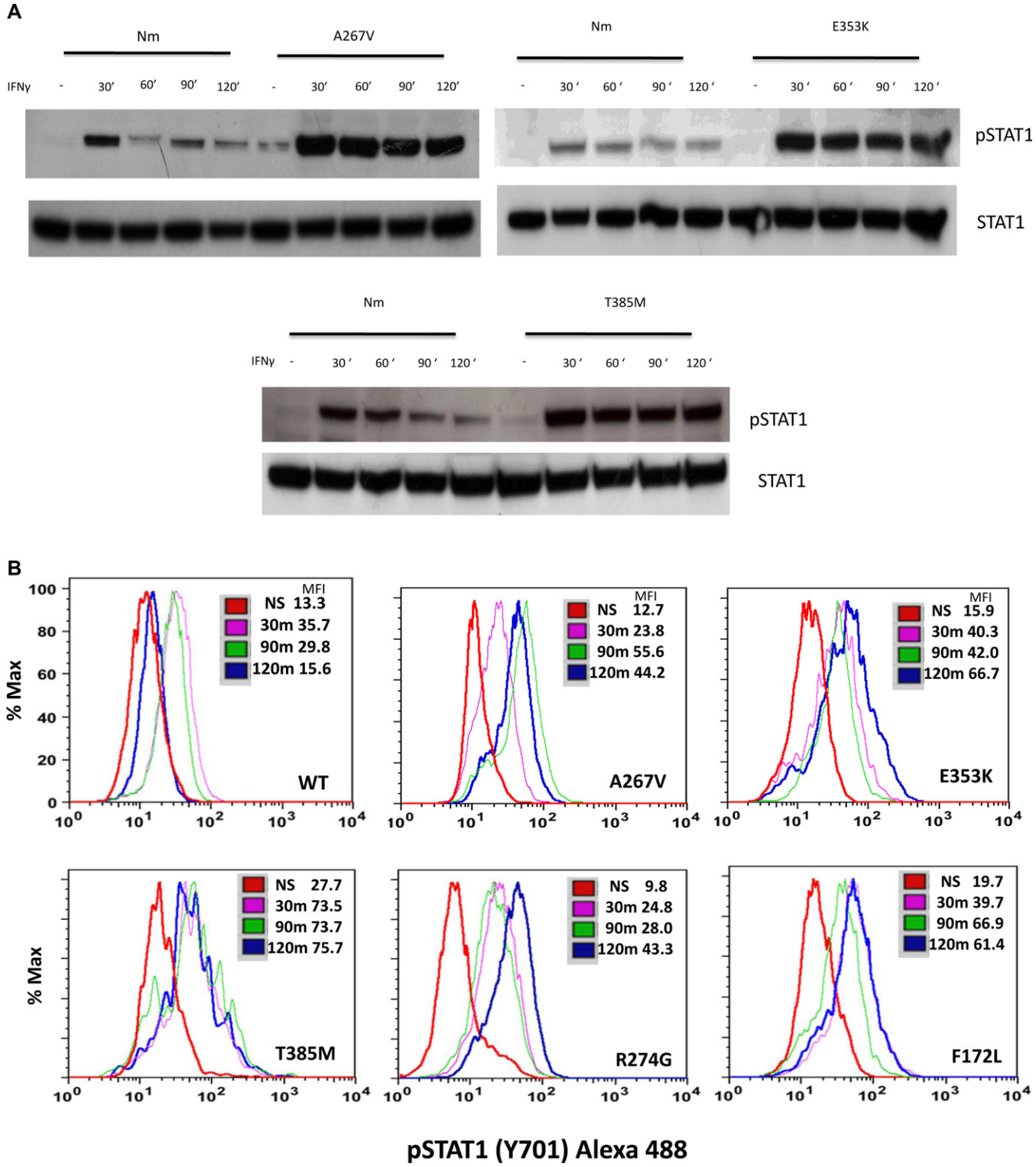

FIG 3. STAT1 mutants lead to delayed dephosphorylation and enhanced luciferase GAS-induced activity. **A,** Dephosphorylation in EBV-B cells from patients and control subjects *(Nm)* stimulated with IFN-γ for the indicated periods. **B,** Dephosphorylation assayed by means of flow cytometry in U3A cells. Results are representative of at least 3 independent experiments. *MFI,* Mean fluorescence intensity; *NS,* nonstimulated. **C,** Transcriptional responses to IFN-γ and IFN-α in U3A cells transfected with STAT1 mutant constructs and when cotransfected with WT STAT1. **D,** U3A cells transfected with L706S showed no negative effect on the mutants A267V and E353K. Data show the mean fold increase relative to the WT nonstimulated specimens from a total of 5 experiments. $*P < .05$ when compared with stimulated WT, respectively. $**P < .01$ compared with L706S.

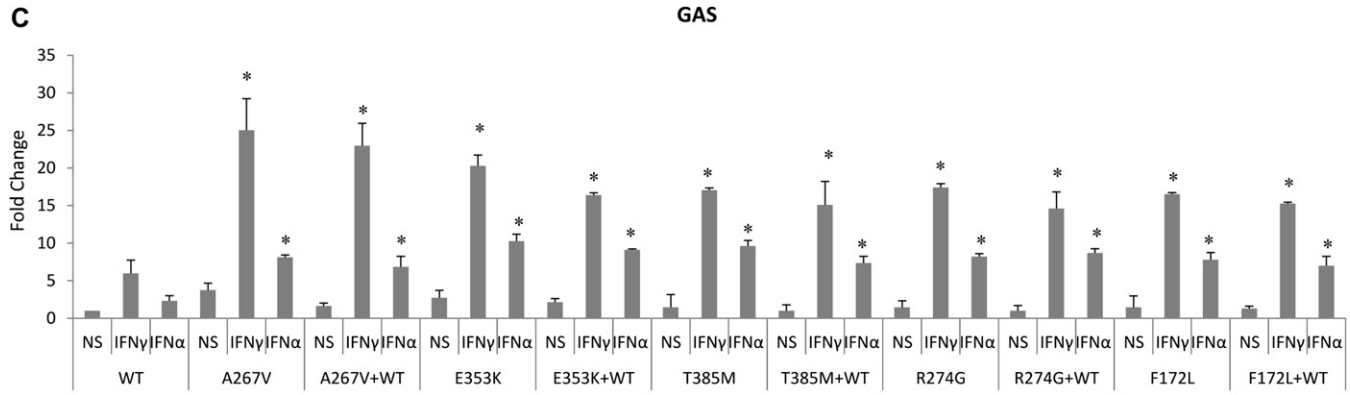

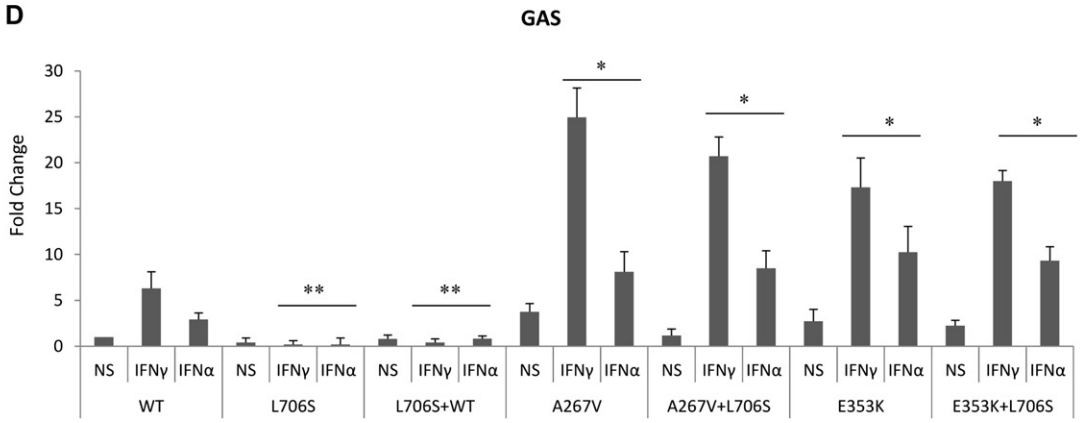

FIG 3. *(Continued)*

disease throughout (Fig 1, *A*), including a new intramedullary spinal cord lesion at T9 with cord edema (Fig 1, *B*).

Patient 2 is a white girl native to Arizona who presented at age 9½ years with 3 weeks of nightly fevers and cough. She had multiple pulmonary nodules, massive necrotic intrathoracic lymphadenopathy with compression of the right mainstem bronchus and vasculature, and lesions of the manubrium and L4, L5, T8, and T9 vertebrae. Coccidioidomycosis was diagnosed by means of serology, leading to fluconazole therapy. Fluconazole was changed to itraconazole, but the pulmonary and intrathoracic lesions continued to enlarge (see Fig E1 and the Results section in this article's Online Repository at www.jacionline.org). At age 13½ years, multiple ring-enhancing lesions appeared in both cerebral hemispheres and the cerebellum. A right subretinal mass thought to be coccidioidal was treated with intraocular amphotericin B without improvement. Despite aggressive treatment with caspofungin, voriconazole, posaconazole, and steroids for inflammatory control, she died of overwhelming *Coccidioides* species infection at 17 years.

Patient 3 is a 21-year-old white man with a lifetime history of recurrent infections; 6 fractures in childhood, including the long and short bones; muscle weakness and atrophy; and bronchiectasis. Thrush appeared at 7 days of life and persisted for 4 years despite topical antifungal therapies. He also had onychomycosis. Fluconazole was started at age 4 years, and fungal infections resolved. At the same age, a single cervical node involved with *Mycobacterium fortuitum* was surgically excised. At age 12 years, he had severe disseminated histoplasmosis, which responded to itraconazole. Since age 15 years, he has had progressive bilateral upper limb muscle atrophy and weakness of unclear cause.

Patient 4 is a 31-year-old man who presented with disseminated histoplasmosis at age 17 years. He had tympanostomy tubes placed as a child without subsequent ear infections. He often had oral sores, and at age 16 years, he was hospitalized for oral candidiasis with probable esophageal involvement. At age 17 years, he had lymphadenopathy, fever, and weight loss caused by histoplasmosis involving the liver, bone marrow, and lymph nodes. At age 30 years, headaches and ataxia led to the discovery of multiple brain lesions. Craniotomy and biopsy confirmed the largest lesion to be *Histoplasma capsulatum*. At age 31 years, brain biopsy demonstrated PML caused by JC virus detected on immunohistochemistry. During treatment with IL-2, he had *Pseudomonas aeruginosa*-induced sepsis and died.

Patient 5 is a 25-year-old woman born to unrelated parents who had disseminated histoplasmosis at age 7 years characterized by fever, hepatosplenomegaly, lymphadenopathy, and dyspnea. *H capsulatum* on lymph node and lung biopsies was successfully treated with itraconazole. At age 8 years, histoplasmosis in sputum associated with dyspnea and lymphadenopathy was successfully retreated with itraconazole. After completion of treatment, she had recurrent oral, cutaneous, and vaginal candidiasis. Neither her siblings nor her parents have fungal infections or autoimmunity.

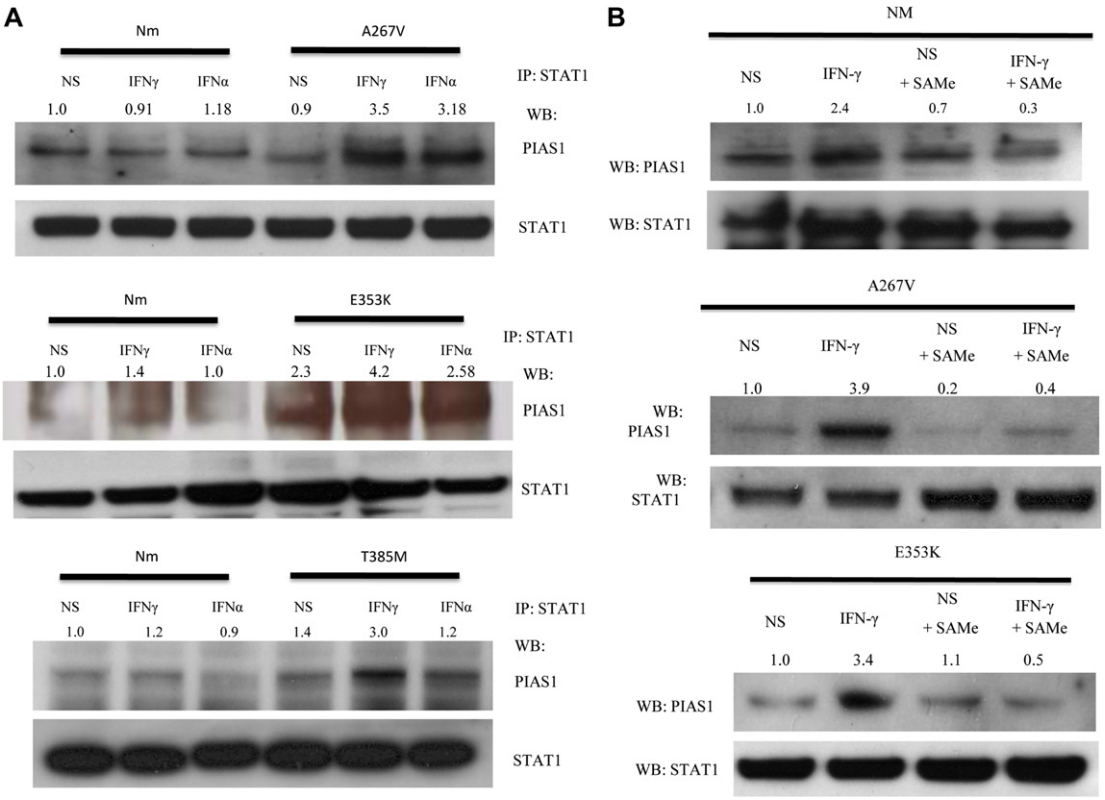

FIG 4. Increased STAT1/PIAS1 association. **A,** After interferon stimulation, cell lysates from EBV-B cells of patients and control subjects *(Nm)* were IP:WB anti-STAT1: anti-PIAS1 antibody. **B,** EBV-B cells treated with SAMe were evaluated as above. Blots are representative of 3 independent experiments for each condition. Numbers are band densities normalized to the nonstimulated samples *(NS).*

STAT1 mutations

Full-length sequencing of *STAT1* genomic and complementary DNA identified *STAT1* heterozygous mutations in each patient. Patient 1 had c.1057G>A, E353K in the DNA-binding domain; patient 2 had c.800C>T, A267V in the coiled-coiled domain[11,12]; patient 3 had c.1154C>T, T385M in the DNA-binding domain; and patient 4 had c.820C>G, R274G and patient 5 had c.514T>C, F172L, both of which were in the coiled-coil domain (Fig 2, *A*). R274G is a different amino acid change at the same location as one previously reported in patients with CMC.[12] In all cases sequencing of full-length cDNA demonstrated equal representation of mutant and WT alleles, indicating stability of the mutant mRNA. None of the patients' parents (patient 4's parents were not tested) carried the identified mutations, nor were these mutations found in dbSNP 132 or the 1000 Genomes Project.

Delayed STAT1 dephosphorylation, enhanced DNA binding, and transactivation

STAT1-deficient U3A cells were transfected with WT and mutant *STAT1* alleles to evaluate the activity of the STAT1 mutant proteins. Immunoblotting confirmed equal expression in transfected cells (Fig 2, *B*).

The STAT1 mutants in patients with histoplasmosis and coccidioidomycosis, as well as F172L (a critical site for STAT1 dephosphorylation),[16] showed enhanced IFN-γ– and IFN-α–induced STAT1 phosphorylation in EBV-B cells (patients 1, 2, and 3: E353K, A267V, and T385M, respectively) and transfected U3As (R274G and F172L) compared with WT cells (see Fig E2, *A*, in this article's Online Repository at www.jacionline.org). Confocal microscopy (see the Results section in this article's Online Repository at www.jacionline.org) confirmed the ability of STAT1 mutants to translocate to the nucleus after activation (Fig E2, *B*). These gain-of-function mutations led to persistent STAT1 phosphorylation for up to 120 minutes, a time at which healthy subjects had almost completely returned to baseline levels (Fig 3, *A*). Experiments with the kinase inhibitor staurosporine (see Fig E2, *C*) and flow cytometry confirmed the impaired dephosphorylation of the mutant proteins (Fig 3, *B*).

STAT1 GAS-binding activity in stimulated EBV-B cells from patients with gain-of-function mutants but not the dominant negative mutant L706S was enhanced in response to interferons when compared with that seen in healthy subjects (see Fig E3, *A*, in this article's Online Repository at www.jacionline.org). Assessment of transactivation response in U3A cells transfected with mutant constructs also showed enhanced activation of the GAS-luciferase reporter after IFN-γ and IFN-α stimulation compared with WT cells (Fig 3, *C*). When WT STAT1 was cotransfected with the mutants, the enhanced activity remained essentially unchanged, confirming the dominant gain of function exerted by the mutant alleles (Fig 3, *C*). Interestingly, cotransfection of U3A cells with these STAT1 mutants along with the L706S dominant negative STAT1 construct showed the gain-of-function mutants to overcome the dominant negative mutant (Fig 3, *D*). The IFN-α–induced transcription activity in cells cotransfected

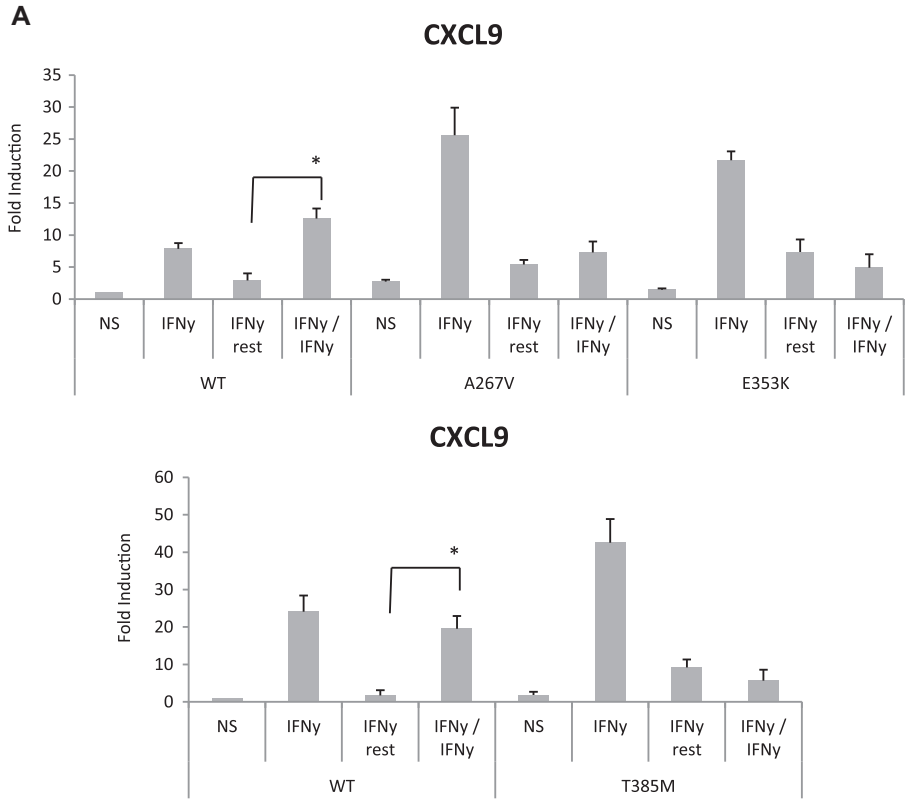

FIG 5. Gene expression: restimulation experiments in transfected U3A cells. Cells were stimulated or not *(NS)* with IFN-γ, washed, and restimulated *(IFN-γ/IFN-γ)* or not *(IFN-γ rest)*. Expression of IFN-γ (*CXCL9* **[A]** and *CXCL10* **[B]**) target genes was evaluated. Results are means ± SDs of 3 independent experiments. *$P < .05$ compared with IFN-γ rest.

with a dependent type I interferon response element (ISRE) was not different than that observed for the WT cells (see Fig E3, *B*).

PIAS1-STAT1 interaction

PIAS1 modulates STAT1 activity, and STAT1/PIAS1 interaction is also reported to be modulated by methylation of STAT1.[17,18] After stimulation with interferons, PIAS1/STAT1 interaction was enhanced in patients' B cells compared with healthy donors when cell lysates were immunoprecipitated for STAT1 and blotted for associated PIAS1 (Fig 4, *A*). Moreover, immunoprecipitated lysates immunoblotted with a mono/dimethylarginine antibody (DMA) showed diminished methyl-STAT1 in stimulated mutant transfected U3A or EBV-B cells compared with normal cells (see Fig E4, *A*, in this article's Online Repository at www.jacionline.org). Treatment of cells with the well-characterized methyl donor S-adenosylmethionine (SAMe; 1600 nmol/L; Sigma-Aldrich, St Louis, Mo), which donates to the terminal nitrogen of arginine residues on target proteins,[19] led to enhanced methyl-associated STAT1 (see Fig E4, *B*), decreased STAT1/PIAS1 association (Fig 4, *B*), and reduced IFN-γ–induced STAT1 phosphorylation compared with that seen in untreated cells (see Fig E4, *C*).

Gene expression

The effects of these novel dominant STAT1 mutations on IFN-γ–inducible target genes (CXC chemokine ligand 9 *[CXCL9]* and *CXCL10 [IP10]*, see Fig E5, *A*, in this article's Online Repository at www.jacionline.org) but not on traditional IFN-α target genes (*MX1* and *ISG15*, see Fig E5, *B*) were enhanced in U3A cells carrying mutant *STAT1* constructs compared with WT *STAT1*. To better understand the connection of STAT1 hyperactivation and impaired response in the IFN-γ axis, we examined whether the hyperresponsiveness induced by these mutations impaired later IFN-γ responses. Transfected U3A cells were stimulated with IFN-γ for 3 hours, washed free of IFN-γ (IFN-γ restimulation), and then restimulated with IFN-γ for an additional 3 hours (IFN-γ/IFN-γ). In these experiments WT STAT1-expressing cells showed clear-cut ability to augment gene expression (*CXCL9* and *CXCL10*) after both stimulation and restimulation. In contrast, mutant *STAT1* cells were able to upregulate their response to the initial IFN-γ stimulation but not restimulation (Fig 5). These results were reproduced when using primary patients' PBMCs restimulated *in vitro* (see Fig E5, *C*). Failure to respond to restimulation with IFN-γ was also observed for the mutations K286I and T288A, which have been described as being associated with CMC alone (see Fig E5, *D*).[12]

We investigated whether PIAS1 plays a role in the impaired gene expression seen after restimulation. Knockdown of PIAS1 (see Fig E6 in this article's Online Repository at www.jacionline.org) in U3A cells (but not control siRNA, data not shown) cotransfected with gain-of-function STAT1 mutants led to near normalization of gene expression after restimulation (Fig 6).

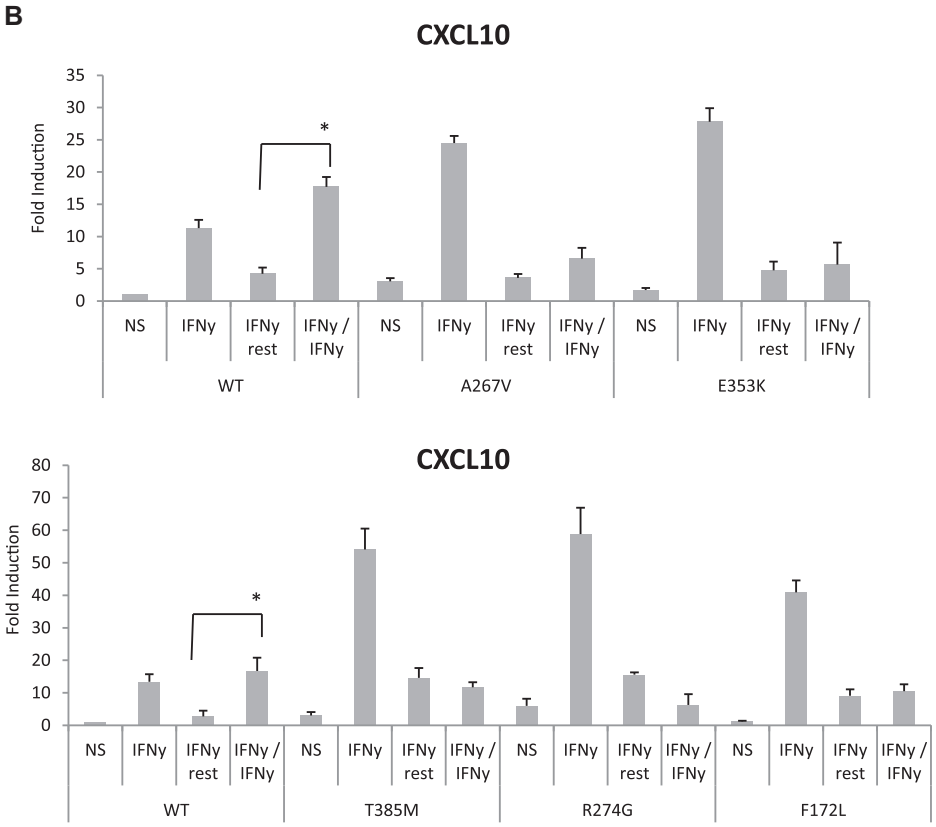

FIG 5. *(Continued)*

Cytokine production and evaluation of T_H17 response

Secretion of proinflammatory cytokines (TNF-α and IL-12p70) was upregulated in patients compared with healthy subjects. The T_H17 response assayed in PBMCs ($CD3^+CD4^+CD45RO^+$ cells) was low for the patients carrying the mutations A267V, E353K, and T385M (see Fig E7 in this article's Online Repository at www.jacionline.org) but not in a patient missing IFN-γ receptor 1 (del*IFNGR1*) or one with disseminated coccidioidomycosis without a recognized mutation, suggesting that defective production of T_H17 cells is not necessary for the development of disseminated dimorphic fungal infection.

DISCUSSION

Genetic defects in the IFN-γ/IL-12 pathway have been found in patients with severe disseminated histoplasmosis and coccidioidomycosis,[3-6] indicating that underlying deficiencies in the same genes that control nontuberculous mycobacteria and *Salmonella* species are also involved in the control of intracellular fungal disease, which was the reason to investigate this pathway in our patients in the first place.

Coccidioidomycosis is endemic in the American Southwest into South America, but most disease is limited and transient. However, dissemination occurs more often in certain ethnic groups, most notably African American and Filipino subjects, suggesting underlying genetic contributions.[20,21] Both of our patients with disseminated coccidioidomycosis also had years of progressive pulmonary involvement without associated lung cavitation. Such chronic manifestations are so distinctly unusual for patients with coccidioidal infection that it might be specifically associated with aberrant STAT1 function. *H capsulatum* occurs worldwide, typically as a limited disease, but disseminated disease signifies immunodeficiency.[22] Extrapulmonary coccidioidomycosis and histoplasmosis have also been described in patients with hyper-IgE syndrome caused by *STAT3* mutations,[23,24] even though infections are less severe.

The mutations we identified in *STAT1* were in the coiled-coil and DNA-binding domains and led to severe fungal infections with or without CMC. Notably, patient 4 also had warts and PML. Recurrent oral herpes virus infections have been reported in STAT1 gain-of-function mutations,[25] as well as severe herpes simplex virus and varicella zoster virus infections (Uzel et al, accompanying submission). The occurrence of viral, mycobacterial, and dimorphic fungal infections with these mutations in *STAT1* suggests a functional overlap of the gain- and loss-of-function mutations, which can converge on the integrity of secondary responses to IFN-γ.

Members of the PIAS family negatively regulate the Janus kinase–STAT pathway and modulate nuclear factor κB signaling and other pathways.[26,27] PIAS1 interacts with the amino terminal domain of STAT1 (amino acids 1-191),[28] where arginine 31 is located, the described site for STAT1 and STAT3 methylation.[17,29,30] PIAS can also act as a SUMO E3 ligase, which might be relevant because STAT1 SUMOylation seems to modulate the transcriptional activity of target genes, the expression of PIAS1-sensitive genes, and the extent of responsiveness to IFN-γ.[31] Chromatin immune precipitation studies on PIAS1-deficient macrophages and transcriptional analysis of cells treated with interferon found increased STAT1 binding to the promoters of PIAS1-sensitive genes (*CXCL9* and *CXCL10*) but not

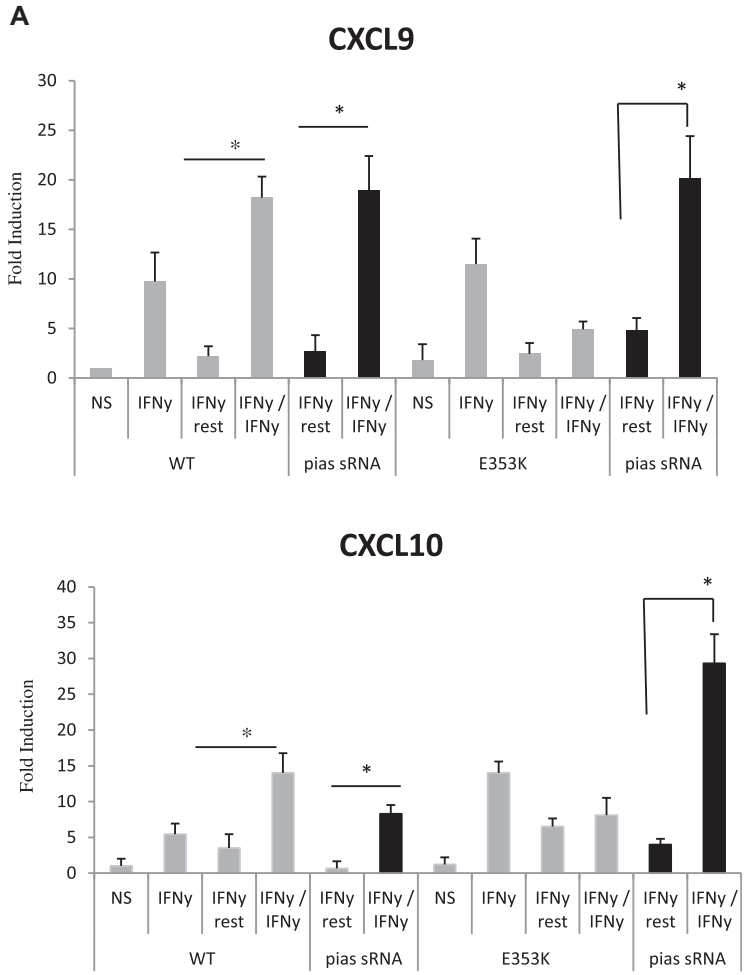

FIG 6. Reduction of PIAS1 modulates the IFN-γ–induced gene response. Evaluation of gene expression in U3A cells cotransfected with WT or mutant STAT1 and with siRNA directed against PIAS1. Cells were treated as described in Fig 5. Restimulated cells = IFN-γ/IFN-γ or PIAS siRNA IFN-γ/IFN-γ. Results are means ± SDs of 3 independent experiments. *NS*, Nonstimulated. *$P < .05$ when compared with IFN-γ rest. **A,** WT and E353K with and without PIAS siRNA. **B,** WT, A267V, and R274G with and without PIAS siRNA.

PIAS1-insensitive genes, indicating a select population of genes regulated by PIAS1.[27,32] Analogously, lysine methylation modifies STAT3-mediated responses.[33] Disruption of K140 caused persistent STAT3 phosphorylation, differentially modulated IL-6–induced gene expression, and downregulation of a subset of genes after restimulation.

Similarly, the *STAT1* mutations we identified did not normally upregulate gene expression after restimulation. Moreover, reduction of PIAS1 in the mutant cells restored the restimulation response to IFN-γ, as observed in WT cells. It is noteworthy that the defect is brought out predominantly by restimulation, suggesting that the occurrence of IFN-γ tachyphylaxis might be central to the defect in this condition.

STAT1/PIAS1 association can be modulated by STAT1 methylation.[17,18,34,35] Treatment of patients' cells with SAMe reduced STAT1/PIAS1 association and decreased STAT1 phosphorylation and restored the restimulation response to IFN-γ *in vitro*. SAMe is a principal biologic methyl donor, the precursor for polyamine biosynthesis, described to overcome hepatitis virus–associated STAT1 hypomethylation.[19,34-36] SAMe might have potential therapeutic uses in patients with *STAT1* mutants.

STAT1 has a critical role in the control of fungal and other infections. Human susceptibility to coccidioidomycosis and histoplasmosis is apparently enhanced by both loss- and gain-of-function mutations in the IFN-γ/IL-12 pathway, likely through mechanisms other than the impaired IL-17 response that predisposes patients to CMC.

We thank Ervand Kristosturyan and Lev Heller for technical assistance and Steven Becker (Biological Imaging Facility/RTB, NIAID/NIH) for assistance with the confocal experiments.

Clinical implications: *STAT1* gain-of-function mutations predispose to disseminated dimorphic fungal infections. Prolonged STAT1 phosphorylation, hypomethylation, and impaired dephosphorylation impair IFN-γ restimulation, leading to apparent tachyphylaxis.

REFERENCES

1. Al-Muhsen S, Casanova JL. The genetic heterogeneity of Mendelian susceptibility to mycobacterial diseases. J Allergy Clin Immunol 2008;122:1043-51.

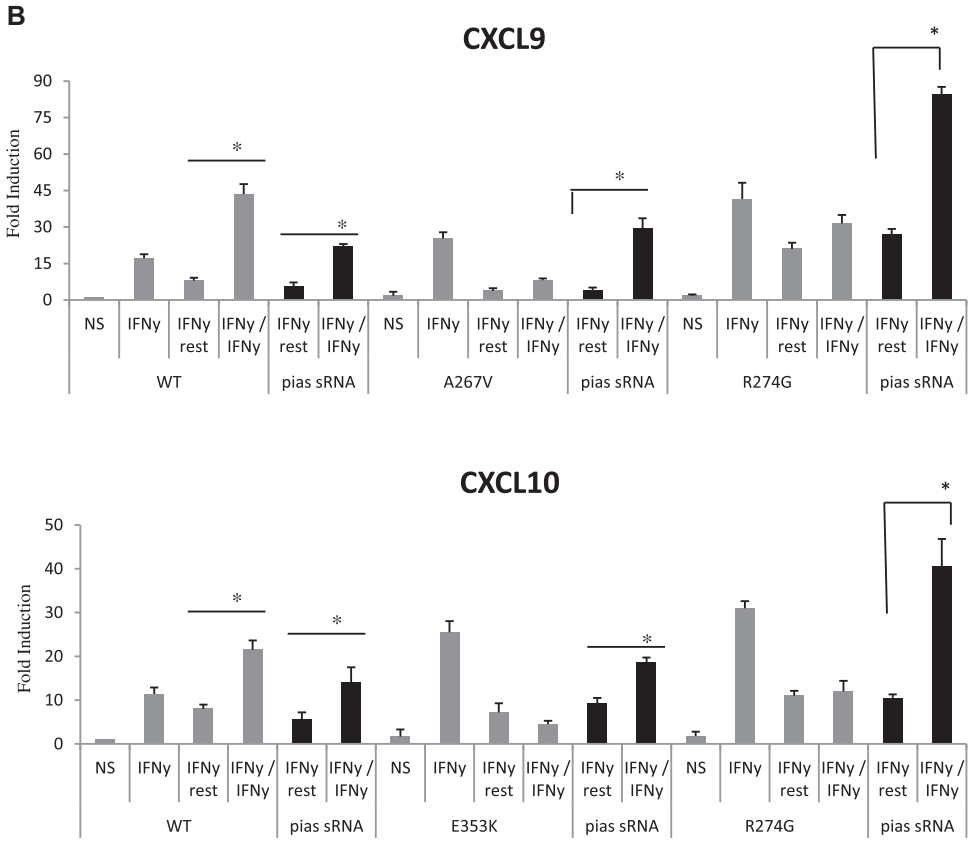

FIG 6. *(Continued)*

2. Haverkamp MH, van Dissel JT, Holland SM. Human host genetic factors in non-tuberculous mycobacterial infection: lessons from single gene disorders affecting innate and adaptive immunity and lessons from molecular defects in interferon-gamma-dependent signaling. Microbes Infect 2006;8:1157-66.
3. Zerbe CS, Holland SM. Disseminated histoplasmosis in persons with interferon-gamma receptor 1 deficiency. Clin Infect Dis 2005;41:e38-41.
4. Moraes-Vasconcelos D, Grumach AS, Yamaguti A, Andrade ME, Fieschi C, de Beaucoudrey L, et al. *Paracoccidioides brasiliensis* disseminated disease in a patient with inherited deficiency in the beta1 subunit of the interleukin (IL)-12/IL-23 receptor. Clin Infect Dis 2005;41:e31-7.
5. Vinh DC, Masannat F, Dzioba RB, Galgiani JN, Holland SM. Refractory disseminated coccidioidomycosis and mycobacteriosis in interferon-gamma receptor 1 deficiency. Clin Infect Dis 2009;49:e62-5.
6. Vinh DC, Schwartz B, Hsu AP, Miranda DJ, Valdez PA, Fink D, et al. Interleukin-12 receptor β1 deficiency predisposing to disseminated Coccidioidomycosis. Clin Infect Dis 2011;52:e99-102.
7. Casanova JL, Holland SM, Notarangelo LD. Inborn errors of human JAKs and STATs. Immunity 2012;36:515-28.
8. Dupuis S, Dargemont C, Fieschi C, Thomassin N, Rosenzweig S, Harris J, et al. Impairment of mycobacterial but not viral immunity by a germline human STAT1 mutation. Science 2001;293:300-3.
9. Chapgier A, Wynn RF, Jouanguy E, Filipe-Santos O, Zhang S, Feinberg J, et al. Human complete Stat-1 deficiency is associated with defective type I and II IFN responses in vitro but immunity to some low virulence viruses in vivo. J Immunol 2006;176:5078-83.
10. Averbuch D, Chapgier A, Boisson-Dupuis S, Casanova JL, Engelhard D. The clinical spectrum of patients with deficiency of signal transducer and activator of transcription-1. Pediatr Infect Dis J 2011;30:352-5.
11. van de Veerdonk FL, Plantinga TS, Hoischen A, Smeekens SP, Joosten LA, Gilissen C, et al. STAT1 mutations in autosomal dominant chronic mucocutaneous candidiasis. N Engl J Med 2011;365:54-61.
12. Liu L, Okada S, Kong XF, Kreins AY, Cypowyj S, Abhyankar A, et al. Gain-of-function human STAT1 mutations impair IL-17 immunity and underlie chronic mucocutaneous candidiasis. J Exp Med 2011;208:1635-48.
13. Tamiya T, Kashiwagi I, Takahashi R, Yasukawwa H, Yoshimura A. Suppressors of cytokine signaling (SOCS) proteins and JAK/STAT pathways. Regulation of T cell inflammation by SOCS1 and SOCS3. Arterioscler Thromb Vasc Biol 2011;31:980-5.
14. Shuai K. Regulation of cytokine signaling pathways by PIAS proteins. Cell Res 2006;16:196-202.
15. Palvimo JJ. PIAS proteins as regulators of small ubiquitin-related modifier (SUMO) modifications and transcription. Biochem Soc Trans 2007;35:1405-8.
16. Zhong M, Henriksen MA, Takeuchi K, Schaefer O, Liu B, ten Hoeve J, et al. Implications of an antiparallel dimeric structure of nonphosphorylated STAT1 for the activation-inactivation cycle. Proc Natl Acad Sci U S A 2005;102:3966-71.
17. Mowen KA, Tang J, Zhu W, Schurter BW, Shuai K, Herschman HR, et al. Arginine methylation of STAT1 modulates IFNalpha/beta-induced transcription. Cell 2001;104:731-41.
18. Zhu W, Mustelin T, David M. Arginine methylation of STAT1 regulates its dephosphorylation by T cell protein tyrosine phosphatase. J Biol Chem 2002;277:35787-90.
19. Anstee QM, Day CP. S-adenosylmethionine (SAMe) therapy in liver disease: a review of current evidence and clinical utility. J Hepatol 2012;57:1097-109.
20. Adam RD, Elliott SP, Taljanovicc MS. The spectrum and presentation of disseminated coccidioidomycosis. Am J Med 2009;122:770-7.
21. Hector RF, Rutherford GW, Tsang CA, Erhart LM, McCotter O, Anderson SM, et al. The public health impact of coccidioidomycosis in Arizona and California. Int J Environ Res Public Health 2011;8:1150-73.
22. Hostoffer RW, Berger M, Clark HT, Schreiber JR. Disseminated *Histoplasma capsulatum* in a patient with hyper IgM immunodeficiency. Pediatrics 1994;94:234-6.
23. Powers AE, Bender JM, Kumánovics A, Ampofo K, Augustine N, Pavia AT, et al. *Coccidioides immitis* meningitis in a patient with hyperimmunoglobulin E syndrome due to a novel mutation in signal transducer and activator of transcription. Pediatr Infect Dis J 2009;28:664-6.
24. Vinh DC, Sugui JA, Hsu AP, Freeman AF, Holland SM. Invasive fungal disease in autosomal-dominant hyper-IgE syndrome. J Allergy Clin Immunol 2010;125:1389-90.
25. Tóth B, Méhes L, Taskó S, Szalai Z, Tulassay Z, Cypowyj S, et al. Herpes in STAT1 gain-of-function mutation [corrected]. Lancet 2012;379:2500.
26. Liu B, Yang R, Wong KA, Getman C, Stein N, Teitell MA, et al. Negative regulation of NF-kappaB signaling by PIAS1. Mol Cell Biol 2005;25:1113-23.
27. Shuai K, Liu B. Regulation of gene activation pathways by PIAS proteins in the immune system. Nat Rev Immunol 2005;5:593-605.

28. Shuai K. Modulation of STAT signaling by STAT-interacting proteins. Oncogene 2000;19:2638-44.
29. Wolf SS. The protein arginine methyltransferase family: an update about function, new perspectives and the physiological role in humans. Cell Mol Life Sci 2009;66:2109-21.
30. Iwasaki H, Kovacic JC, Olive M, Beers JK, Yoshimoto T, Crook MF, et al. Disruption of protein arginine N-methyltransferase 2 regulates leptin signaling and produces leanness in vivo through loss of STAT3 methylation. Circ Res 2010;107:992-1001.
31. Begitt A, Droescher M, Knobeloch KP, Vinkemeier U. SUMO conjugation of STAT1 protects cells from hyperresponsiveness to IFNγ. Blood 2011;118:1002-7.
32. Liu B, Mink S, Wong KA, Stein N, Getman C, Dempsey PW, et al. PIAS1 selectively inhibits interferon-inducible genes and is important in innate immunity. Nat Immunol 2004;5:891-8.
33. Yang J, Huang J, Dasgupta M, Sears N, Miyagi M, Wang B, et al. Reversible methylation of promoter-bound STAT3 by histone-modifying enzymes. Proc Natl Acad Sci U S A 2010;107:21499-504.
34. Li J, Chen F, Zheng M, Zhu H, Zhao D, Liu W, et al. Inhibition of STAT1 methylation is involved in the resistance of hepatitis B virus to interferon alpha. Antiviral Res 2010;85:463-9.
35. Feld JJ, Modi AA, El-Diwany R, Rotman Y, Thomas E, Ahlenstiel G, et al. S-Adenosylmethionine improves early viral responses and interferon-stimulated gene induction in hepatitis C nonresponders. Gastroenterology 2011;140:830-9.
36. Filipowicz M, Bernsmeier C, Terracciano L, Duong FH, Heim MH. S-adenosylmethionine and betaine improve early virological response in chronic hepatitis C patients with previous nonresponse. PLoS One 2010;5:e15492.

METHODS

Reagents

Anti-pSTAT1 tyrosine (Tyr)701 and anti-total STAT1 (N-terminal domain) antibodies were from Cell Signaling Technology (Danvers, Mass); anti-PIAS1 was from Santa Cruz Biotechnology (Santa Cruz, Calif); monoclonal DMA was from Abcam (Cambridge, Mass); methylthioadenosine and SAMe (AdoMet) were from Sigma-Aldrich; FCS was from Gibco BRL (Carlsbad, Calif); human IFN-γ was from R&D Systems (Minneapolis, Minn); and IFN-α2b was from PBL Biomedical Laboratories (Piscataway, NJ). Complete Dulbecco modified Eagle medium (Gibco) was supplemented with 10% FCS, 2 mmol/L L-glutamine, and antibiotics.

Confocal microscopy

U3A cells were seeded in 12-well plates (Costar, Sigma-Aldrich), followed by transfection with plasmids encoding WT STAT1 and its mutants or GFP-tagged constructs in the presence of lipofectamine (Invitrogen). The following day, culture media were replaced, and cells were either untreated or treated with IFN-γ (400 IU/mL) for 30 minutes. Cells were then fixed with 4% paraformaldehyde and permeabilized with 0.2% (wt/vol) Triton X-100 in PBS. Cover slips were incubated with the mouse anti-human STAT1 (BD Biosciences, Franklin Lakes, NJ), followed by a secondary staining with goat anti-mouse IgG conjugated to Alexa Flour 568. The nuclei were stained with 4′-6-diamidino-2-phenylindole dihydrochloride (Invitrogen). Cover slips were mounted on slides with the Fluoromount G (Electron Microscopy Sciences, Hatfield, Pa). Colocalization studies were done with the Leica SP5 confocal microscope (Leica Microsystems, Exton, Pa) using a 63× oil immersion objective NA 1.4. The fluorochromes were excited with a UV laser at 405 nm for 4′-6-diamidino-2-phenylindole dihydrochloride, an Argon laser at 488 nm for GFP, and a DPSS laser at 561 nm for the Alexa Fluor 568. The channels were collected sequentially, and the data were analyzed with Leica software (Buffalo Grove, Ill).

Immunoprecipitation and immunoblotting

EBV-B or transfected U3A cells were lysed in buffer (Cell Signaling) containing protease and phosphatase inhibitors (Calbiochem, Gibbstown, NJ). After 30 minutes of incubation on ice, samples were sonicated, and equal amounts of protein were run on a 10% SDS polyacrylamide gel and subsequently transferred to a polyvinylidene difluoride membrane (Invitrogen). After blocking, the membranes were incubated with primary antibody (1:1,000 dilution), as indicated. Membranes were washed and incubated for an additional hour in horseradish peroxidase–conjugated secondary antibody, and signal was detected with an enhanced chemiluminescence system (ECL; Amersham Biosciences, Piscataway, NJ). Blots were stripped and reprobed with total STAT1 or anti-tubulin antibodies to assess protein loading among samples. For immunoprecipitation, cell lysates were incubated with specific anti-STAT1 antibody and protein G–Sepharose (Amersham Biosciences) overnight at 4°C, and immunoreactive proteins were resolved by means of WB. Band densities were measured with ImageJ software (National Institutes of Health, Bethesda, Md) and normalized to the nonstimulated samples.

Reporter gene assay

U3A cells were cotransfected with WT and/or mutant STAT1 expression constructs along with a plasmid containing tandem interferon-response elements (GAS and ISRE) driving a luciferase reporter gene (1 μg, Panomics). A Renilla expression vector was cotransfected to measure transfection efficiency. After overnight incubation, the media were replaced, and cells were stimulated with human IFN-γ or IFN-α2b (1000 IU/mL) for 6 hours. Cells were resuspended in lysis buffer, and luciferase activity was evaluated by using a dual luciferase assay (Promega). Experiments were done in triplicate, and relative luciferase units were corrected for Renilla activity. Data are expressed as the fold increase in response to interferon over the WT unstimulated samples.

Evaluation of STAT1 activation

STAT1 tyrosine (Y701) phosphorylation (pSTAT-1) was assayed in U3A and EBV-B cells stimulated with IFN-γ (400 IU/mL) or IFN-α (1000 IU/mL). For evaluation of dephosphorylation, kinetic evaluation of STAT1 activation was assayed in cells stimulated with IFN-γ from 30 to 120 minutes. In parallel experiments cells were stimulated with IFN-γ (30 minutes), followed by the addition of staurosporine (500 nmol/L, Calbiochem) and continued incubation for the indicated time periods. Cell lysates were recovered and analyzed by means of WB.

Flow cytometric analysis of dephosphorylation was assayed on transfected U3A cells stimulated as above, fixed, and permeabilized in methanol. Cells were stained for total and phosphorylated (pY701) STAT1 (Alexa Fluor 647– and Alexa Fluor 488–conjugated antibodies, BD Biosciences), and phosphorylation levels were assessed in the gated STAT1-positive cells. Data were collected with a FACSCaliber (BD Biosciences) and analyzed with FlowJo software (TreeStar, Ashland, Ore).

Nuclear complex binding

Nuclear extracts from transfected U3A cells, as well as from patients' and control EBV-B cells, stimulated for 30 minutes with IFN-γ (400 IU/mL) or IFN-α (1000 IU/mL), were prepared by using the Panomics kit (Panomics). For determination of DNA-binding activity, an ELISA-like colorimetric assay (TRANSAM; Active Motif, Carlsbad, Calif) was used. The samples were added to an ELISA plate coated with a STAT1-binding oligonucleotide derived from the GAS sequence and processed according to the manufacturer's protocol. After the colorimetric reaction, the absorbance was measured on a spectrophotometer at 450 nm.

STAT1 activation and evaluation of T_H17 response

Flow cytometric analysis of dephosphorylation was assayed on transfected U3A cells stimulated with IFN-γ (30-120 minutes), fixed, and permeabilized in methanol. Cells were stained for total (Alexa Fluor 647–conjugated anti-STAT1) and phosphorylated pY701 STAT1 (Alexa Fluor 488–conjugated anti-pSTAT1, BD Biosciences). Levels of STAT1 phosphorylation were assessed in the cells gated for the expression of total STAT1. Experiments were performed on fresh or frozen PBMCs obtained from patients and healthy donors to evaluate the T_H17 response. In addition, cells obtained from 2 other patients with disseminated coccidioidomycosis, one carrying an 818del4/partial dominant del *IFNGR1* mutation and one of unknown cause, were assayed. Cells (10^6/mL) were stimulated or not with phorbol 12-myristate 13-acetate (20 ng/mL) and ionomycin (1 μmol/L, Calbiochem) in the presence of brefeldin A (1 μg/mL, Sigma) for 6 hours at 37°C. For intracellular cytokine staining, cells were stained with Live/Dead Fixable Aqua Dead Cell Stain Kit (Invitrogen) and then for extracellular antigens with CD8 APC-H7, CD3 AF700 (BD Biosciences), CD45RO TRPE, and CD27 PeCy5 (Beckman Coulter, Fullerton, Calif) for 30 minutes. Cells were fixed with 4% paraformaldehyde, permeabilized, and stained with CD4 Pe-Cy7, IL-2 fluorescein isothiocyanate, IL-17A phycoerythrin, IFN-γ V450 (all from BD Biosciences), and IL-22 allophycocyanin (R&D Systems) for 30 minutes, washed, and run on a BD LSR Fortessa. Data were collected with a FACSCaliber (BD Biosciences) and analyzed with FlowJo software (TreeStar) by gating on $Live^+CD3^+CD4^+CD8^-CD45RO^+CD27^-$ cells.

RESULTS

Patients

We investigated 5 patients referred for disseminated fungal disease. Patient 1 is a Hispanic female native of Arizona with no relevant previous or family history who presented at age 14 years with extensive persistent tinea capitis and kerion caused by *T tonsurans*. At age 17 years, she presented with prolonged cough, a painless right neck mass, fatigue, and weight loss. CT demonstrated multiple nodules throughout both lung fields with a large consolidation in the right lung, extensive mediastinal lymphadenopathy, right paratracheal adenopathy, and an abscess in the right sternocleidomastoid, which showed coccidioidal spherules. The coccidioidal IgG titer determined by using complement fixation was 1:16. Cerebrospinal fluid (CSF) test and bone scan results

were unremarkable. She received fluconazole and then itraconazole, but 8 months later, she had progressive disease, as evinced by nasal lesion, enlarging cervical and supraclavicular lymphadenopathy, and an increasing *Coccidioides* species titer (1:32). CT scans confirmed diffuse progression with new osteomyelitis at vertebral bodies C6 through T5 and multiple lesions throughout the liver and spleen. She received L-AmB and voriconazole and then posaconazole. Clinical improvement lasted about 18 months. At age 20 years, a new *Coccidioides* species–induced skin lesion developed that was associated with anorexia and weight loss. Posaconazole and L-AmB were restarted. L-AmB was replaced by caspofungin after 2 months, but MRI demonstrated progressive disease throughout, including a new intramedullary spinal cord lesion at T9 with cord compression.

Patient 2 is a white girl native to Arizona who presented at age 9½ years with 3 weeks of nightly fevers and cough. She had multiple pulmonary nodules, massive necrotic intrathoracic lymphadenopathy with compression of the right mainstem bronchus and vasculature, and lesions of the manubrium and L4, L5, T8, and T9 vertebrae. Coccidioidomycosis was diagnosed by means of serology, leading to fluconazole therapy. She was stable for approximately 1½ years on fluconazole, but fevers recurred with left supraclavicular coccidioidal lymphadenopathy; CSF was unremarkable. Ten months later, MRI for headaches showed a 9-mm enhancing lesion in the right temporal lobe. CSF analysis again was unremarkable. Fluconazole was changed to itraconazole, but the pulmonary and intrathoracic lesions continued to enlarge (Fig E1). At 13½ years, multiple ring-enhancing lesions appeared in both cerebral hemispheres and the cerebellum. CSF was normal, but serum coccidioidal titers had increased from 1:16 to 1:32. Subsequent fevers, hoarseness, erosion of the left supraclavicular lymph node through the skin, left navicular and cuboid *C immitis* osteomyelitis, and a new thyroid nodule led to use of voriconazole. At age 15 years, left vocal cord paralysis was caused by progression of intrathoracic disease. L-AmB was added and subsequently posaconazole. Progressive disease with loculated pleural effusion led to adjunctive IFN-γ (50 $\mu g/m^2$), which exacerbated fevers and fatigue without clinical improvement. A right retinal mass thought to be coccidioidal was treated with intraocular amphotericin B without improvement. Despite aggressive treatment with caspofungin, voriconazole, posaconazole, and steroids for inflammatory control, she died of overwhelming *Coccidioides* species infection at age 17 years. No autopsy was performed. Her only past medical history was an episode of suspected viral croup at age 18 months requiring brief hospitalization. There is no family history of significant infections or immunodeficiencies.

Patient 3 is a 21-year-old white man with a lifetime history of recurrent infections; 6 fractures in childhood, including the long and short bones; muscle weakness and atrophy; and bronchiectasis. Thrush appeared at 7 days of life and persisted for 4 years despite topical antifungal therapies. He also had onychomycosis. Fluconazole started at age 4 years, and fungal infections resolved. At the same age, a single cervical node involved with *M fortuitum* was surgically excised. He remained well until age 12 years, when he had severe disseminated histoplasmosis, which responded to itraconazole. At age 15 years, he began having gradual bilateral upper limb muscle atrophy and weakness of unclear cause. He has protective titers to tetanus, diphtheria, *Haemophilus influenzae B*, varicella zoster, and pneumococcus. He has had 2 episodes of shingles and multiple pneumonias.

Patient 4 is a 31-year-old man who had disseminated histoplasmosis initially diagnosed at age 17 years. He had tympanostomy tubes placed as a child without subsequent ear infections. He often had oral sores, and at age 16 years, he was hospitalized for oral candidiasis with probable esophageal involvement. At age 17 years, he had lymphadenopathy, fever, and weight loss caused by histoplasmosis involving the liver, bone marrow, and lymph nodes. HIV results were negative. Amphotericin B for 6 weeks, followed by fluconazole, was associated with relapses that responded to intensified treatment. At 23 years of age, he received a diagnosis of common variable immunodeficiency. Despite intravenous immunoglobulin, he had recurrent thrush, onychomycosis, and warts on his hands. He had 2 episodes of *Salmonella* species bacteremia. At 24 years of age, he had type 1 diabetes mellitus requiring insulin. A bone marrow biopsy specimen at 25 years was negative for *H capsulatum*.

At age 30 years, headaches and ataxia led to the discovery of multiple brain lesions. Craniotomy and biopsy confirmed the largest lesion to be *H capsulatum*; amphotericin B (AmBisome) led to improvement. At age 31 years, his headaches and ataxia worsened with dysarthria. Bone marrow showed no overt abnormality and no *H capsulatum*. An MRI scan of the brain showed some increase in lesions throughout the right frontal cortex, thalami, midbrain, and cerebellum. Brain biopsy demonstrated PML with JC virus on immunohistochemistry. During treatment with IL-2, he had *Pseudomonas aeruginosa*–induced sepsis and died. The patient had a son, 6 years of age, with hypothyroidism and recurrent thrush and a daughter, 4 years of age, with molluscum contagiosum, oral ulcers, and recurrent thrush; neither have been tested genetically.

Patient 5, a 25-year-old woman born to unrelated parents, had disseminated histoplasmosis at age 7 years characterized by fever, hepatosplenomegaly, lymphadenopathy, and dyspnea. *H capsulatum* was detected on lymph nodes and lung biopsy specimens, which was successfully treated with itraconazole. At age 8 years, histoplasmosis was found in sputum associated with dyspnea and lymphadenopathy and was successfully retreated with itraconazole. After completion of itraconazole, she had recurrent oral, cutaneous, and vaginal candidiasis. At age 14 years, she received a diagnosis of subclinical hypothyroidism (increased thyroid-stimulating hormone levels), and at age 24 years, she had ovarian failure. Neither her siblings nor her parents have fungal infections or autoimmunity.

Delayed STAT1 dephosphorylation, enhanced DNA binding, and transactivation

STAT1 mutants showed enhanced IFN-γ– and IFN-α–induced STAT1 phosphorylation in EBV-B cells (available for patients 1, 2, and 3) compared with cells from normal donors (Fig E2, *A*). Confocal microscopy confirmed the ability of STAT1 mutants to translocate to the nucleus after activation (Fig E2, *B*).

Dephosphorylation in patients' EBV-B cells showed persistent STAT1 phosphorylation for up to 120 minutes. Experiments with the kinase inhibitor staurosporine confirmed the impaired dephosphorylation of mutant proteins, whereas cells from healthy subjects had almost completely returned to baseline phosphorylation (Fig E2, *C*).

DNA-binding activity was assayed after stimulation with IFN-γ or IFN-α (1000 IU/mL for 30 minutes). STAT1 GAS-binding activity in stimulated EBV-B cell lysates from patients

with gain-of-function mutations but not the dominant negative mutant L706S was enhanced in response to interferons (mean fold induction: 3.1 ± 0.79 and 2.84 ± 0.47, respectively) compared with healthy subjects (Fig E3, *A*). The transactivation response assayed in U3A cells cotransfected with mutant constructs along with ISRE showed the IFN-α–induced transcription activity was not different than that observed for the WT cells (Fig E3, *B*).

PIAS/STAT1 interaction

Posttranslational modifications, such as methylation and SUMOylation, have both been linked to delayed STAT1 dephosphorylation. STAT1/PIAS1 interaction was also reported to be modulated by methylation of STAT1. STAT1 was immunoprecipitated from transfected U3A cells after stimulation with IFN-γ and immunoblotted with a DMA antibody to evaluate protein methylation. As shown in Fig E4, *A*, U3A cells transfected with the mutant constructs or EBV-B cells from patients had less methyl-STAT1 in response to interferon than WT U3A or normal B cells. Treatment of cells with the methylation inhibitor methylthioadenosine confirmed the ability to detect lower levels of methylated STAT1 in treated cells (data not shown).

Previous studies have shown that treatment of cells *in vitro* with SAMe (or AdoMet), a well-characterized methyl donor to the terminal nitrogen of arginine residues of target proteins, is able to overcome hepatitis virus–associated STAT1 hypomethylation. In our study EBV-B cells pretreated with SAMe (1600 nmol/L) and stimulated with IFN-γ showed enhanced methylated STAT1 and lower PIAS1/STAT1 association (Fig E4, *B*). STAT1/PIAS1 interaction is also reported to be modulated by methylation of STAT1.[E1,E2] Treatment of cells with SAMe also reduced IFN-γ–induced STAT1 phosphorylation (Y701) compared with untreated cells (Fig E4, *C*).

Gene expression

We examined the effects of these novel dominant STAT1 mutations on interferon-inducible genes. The expression of IFN-γ target genes (CXC chemokine ligand 9 *[CXCL9]* and *CXCL10 [IP10]*) in mutant transfected U3A cells was enhanced compared with WT transfectants (Fig E5, *A*). On the other hand, the induced response of the traditional IFN-α target genes *MX1* and *ISG15* was not different when compared with that in WT cells (Fig E5, *B*). In contrast, mutant *STAT1* cells were unable to upregulate gene response after restimulation. These results were reproduced with primary patients' PBMCs restimulated *in vitro* (Fig E5, *C*).

We investigated whether PIAS1 plays a role in the impaired gene expression seen after restimulation. Knockdown of PIAS1 (Fig E6) in U3A cells was achieved by using Target pool siRNA (Dharmacon, Lafayette, Colo). Near normalization of gene expression after restimulation reinforces the critical role that PIAS1 plays in the impaired mutant response to IFN-γ.

Cytokine production and evaluation of T_H17 response

In vitro response in patients' PBMCs was assessed after cell stimulation (48-hour culture) with LPS or LPS plus IFN-γ. Secretion of proinflammatory cytokines (TNF-α and IL-12p70) induced by LPS was upregulated by IFN-γ (5- to 10-fold), which was somewhat higher than the responses of normal donors (4-fold). IFN-γ production induced by phorbol 12-myristate 13-acetate plus ionomycin (percentage of positive cells, Fig E7) was preserved.

T_H17 response assayed in PBMCs ($CD3^+CD4^+CD45RO^+$ cells) was lower for the mutant A267V, as previously reported, for E353K and was strikingly diminished for T385M (Fig E7). For comparison, a patient missing IFN-γ receptor 1 (del *IFNGR1*) and one with disseminated coccidioidomycosis without a recognized mutation had normal levels of IL-17–producing cells.

REFERENCES

E1. Hostoffer RW, Berger M, Clark HT, Schreiber JR. Disseminated *Histoplasma capsulatum* in a patient with hyper IgM immunodeficiency. Pediatrics 1994;94:234-6.

E2. Powers AE, Bender JM, Kumánovics A, Ampofo K, Augustine N, Pavia AT, et al. *Coccidioides immitis* meningitis in a patient with hyperimmunoglobulin E syndrome due to a novel mutation in signal transducer and activator of transcription. Pediatr Infect Dis J 2009;28:664-6.

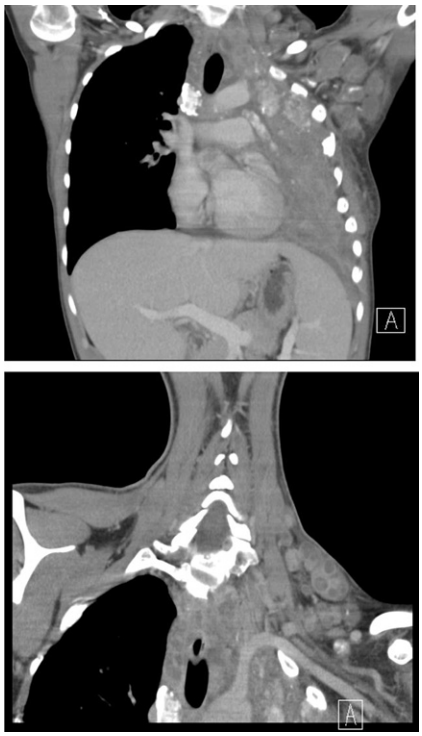

FIG E1. Patient 2: extensive left hemithoracic and nodal involvement with *C immitis*. Right ocular and cerebral involvement are not shown.

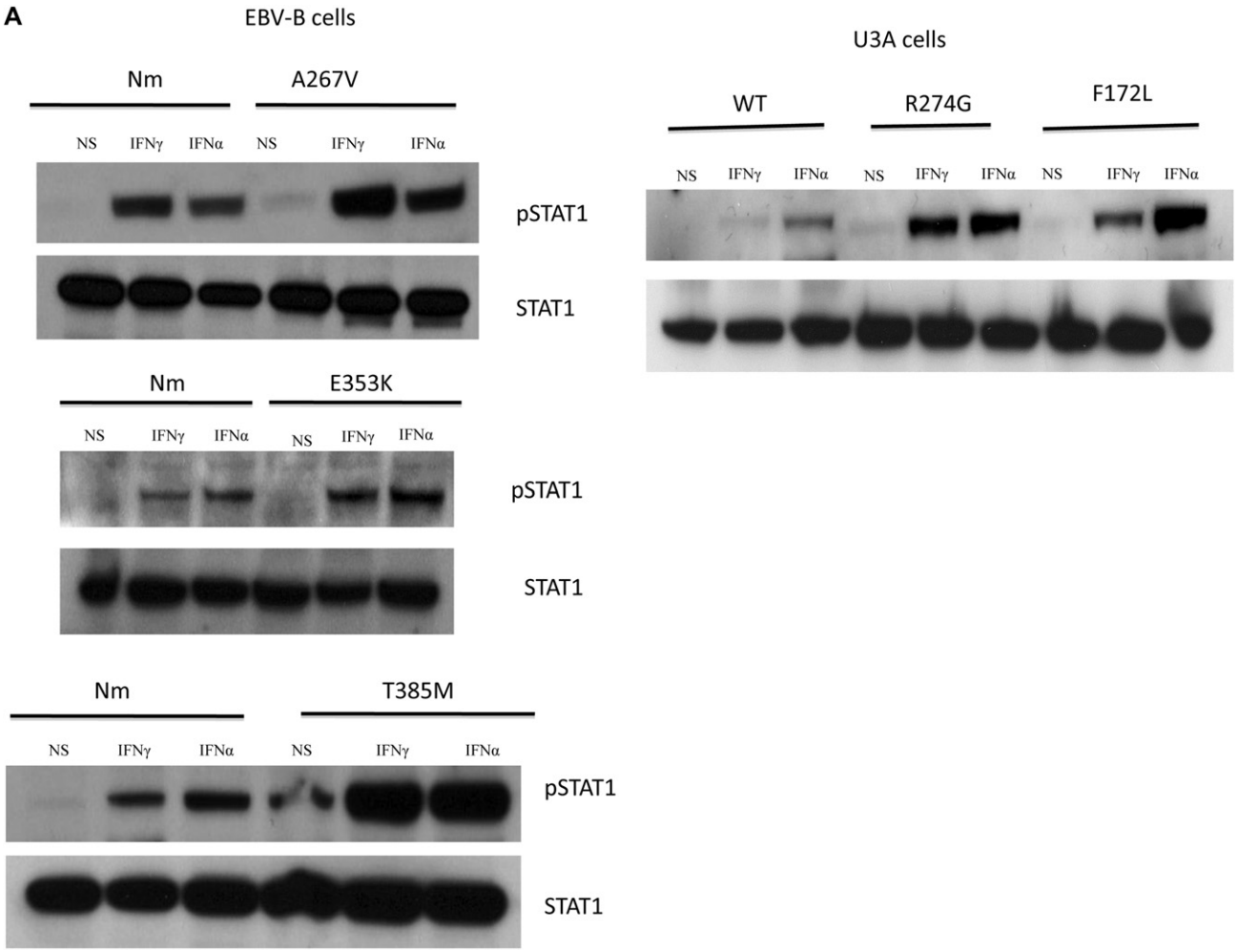

FIG E2. A, EBV-B cells obtained from patients with STAT1 mutations and healthy donors *(Nm)* and transfected U3A cells were stimulated with IFN-γ or IFN-α (15 minutes). Cell lysates were analyzed by means of WB. **B,** Nuclear translocation of STAT1 proteins in IFN-γ–stimulated U3A cells *(overlay image)*: *(1)*, GFP-tagged constructs; *(2)*, secondary staining with Alexa Fluor 568. **C,** Dephosphorylation in EBV-B cells from patients and control subjects stimulated with IFN-γ for the indicated periods with staurosporine added to the remaining wells. Membranes were blotted for pSTAT1, stripped, and reprobed with anti-total STAT1.

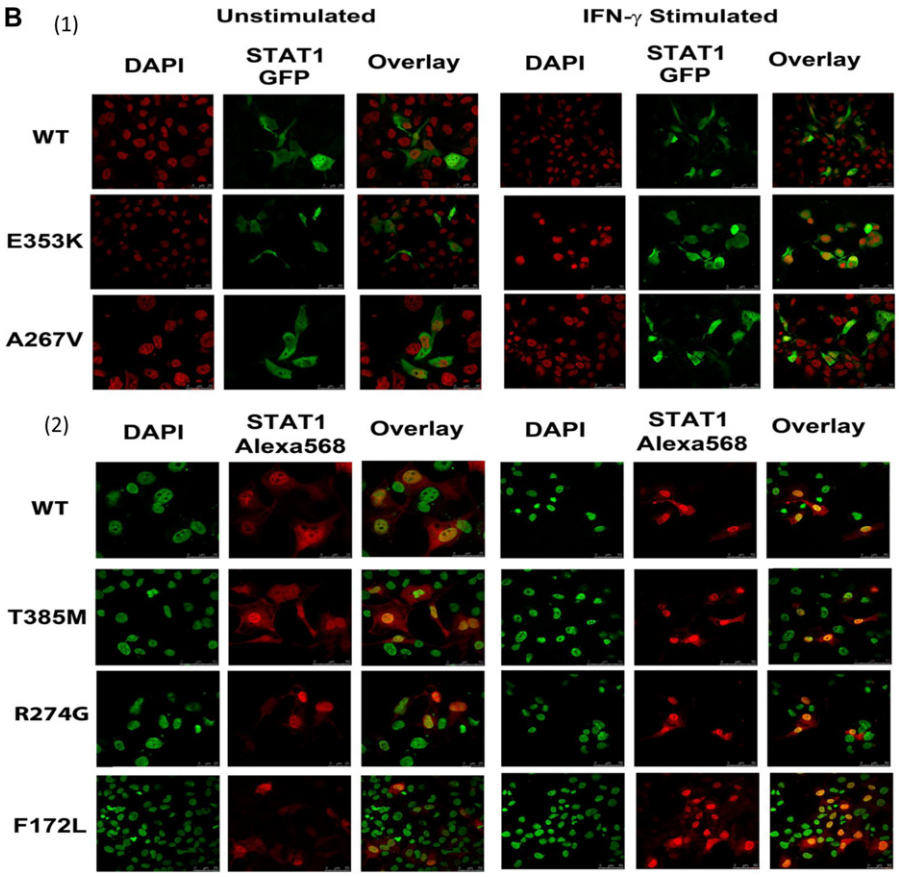

FIG E2. *(Continued)*

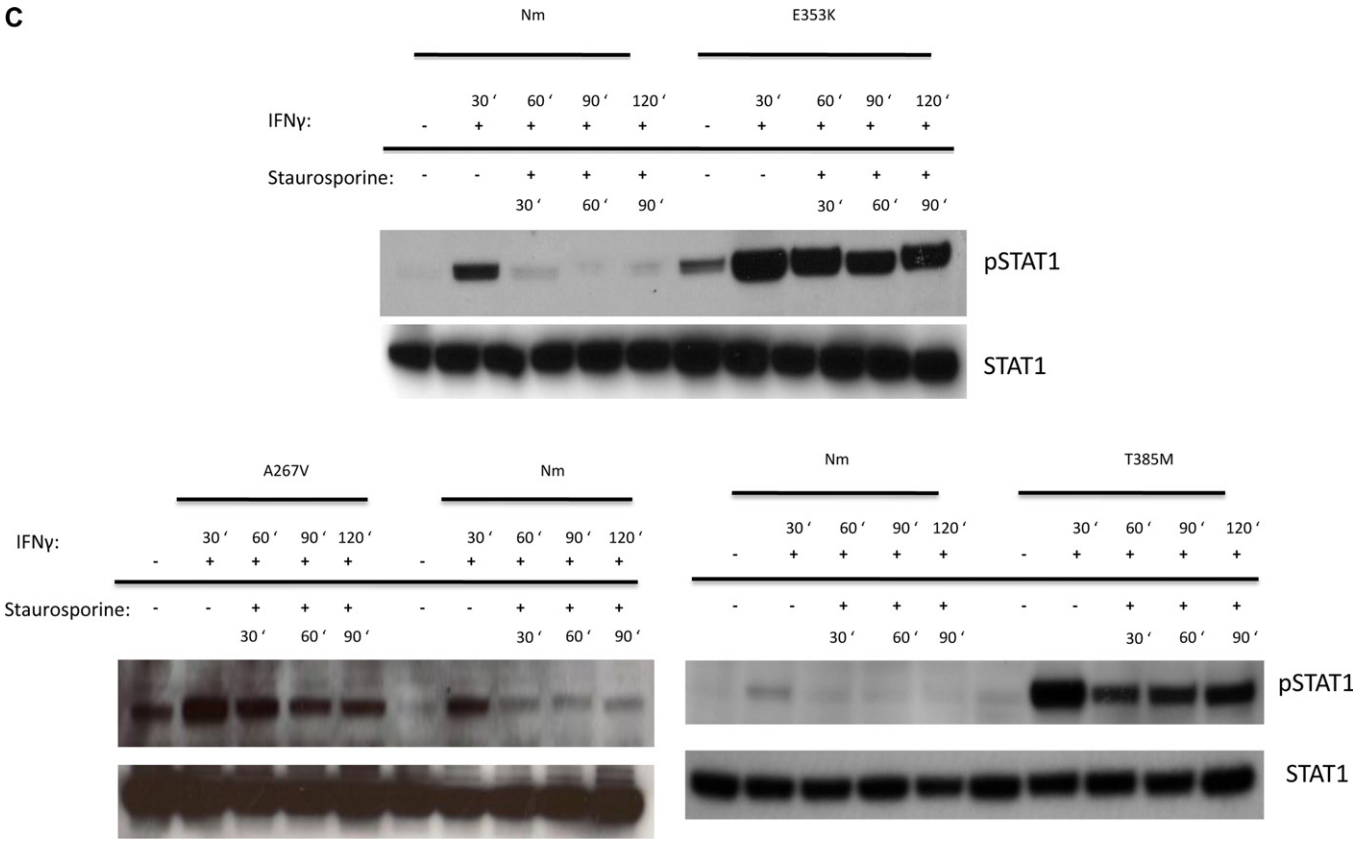

FIG E2. *(Continued)*

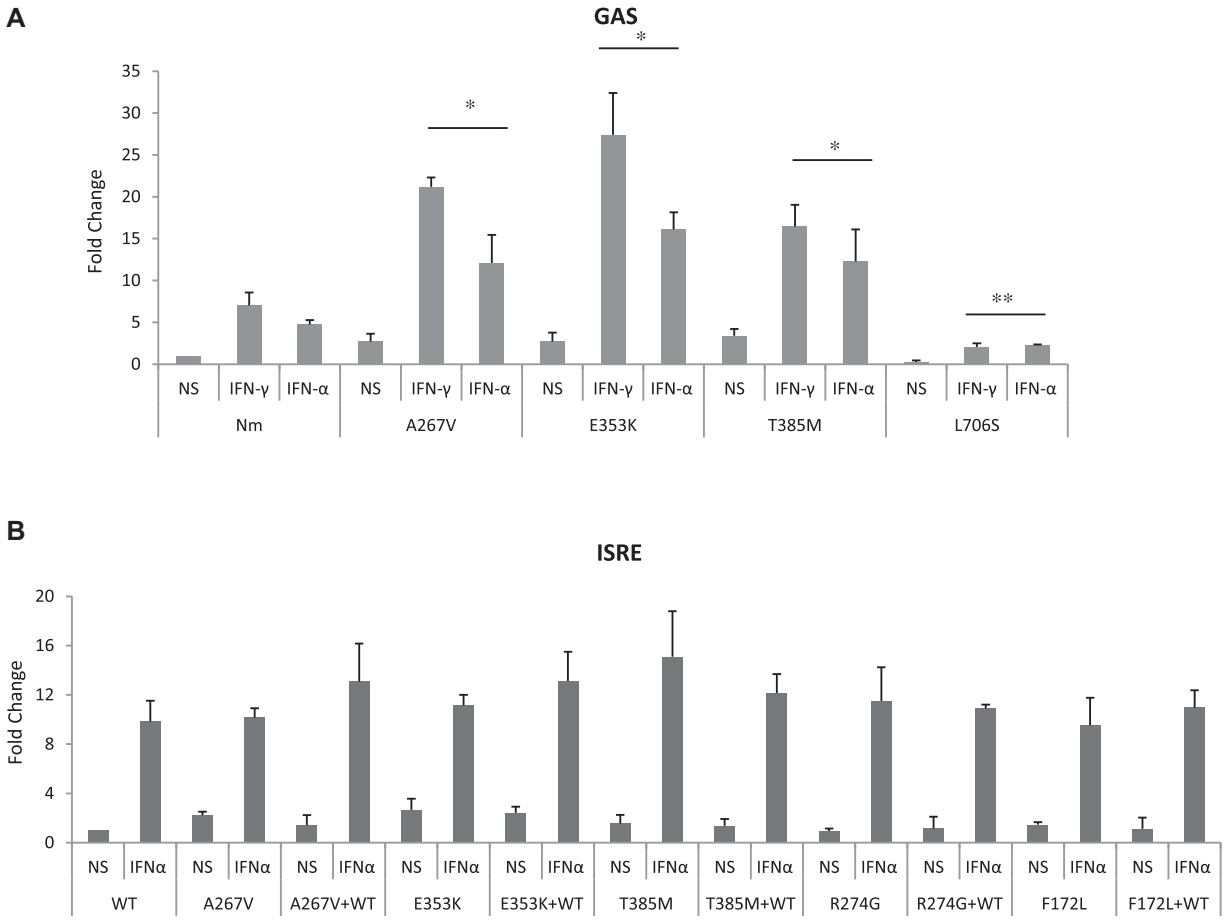

FIG E3. A, STAT1 DNA-binding GAS activity assayed in EBV-B cells from patients and healthy control subjects *(Nm)*. Data are the mean fold increase in the stimulated wells relative to the WT unstimulated cells *(NS)* for 4 independent experiments. *Significant difference ($P < .05$) when compared with stimulated WT cells (IFN-γ or IFN-α, respectively). **$P < .01$ for all mutant constructs compared with L706S. **B,** U3A cells transfected with the luciferase ISRE reporter plasmid together with STAT1 mutant constructs alone or cotransfected with WT STAT1. Similar responses were seen in mutant transfected cells compared with WT cells when stimulated with IFN-α.

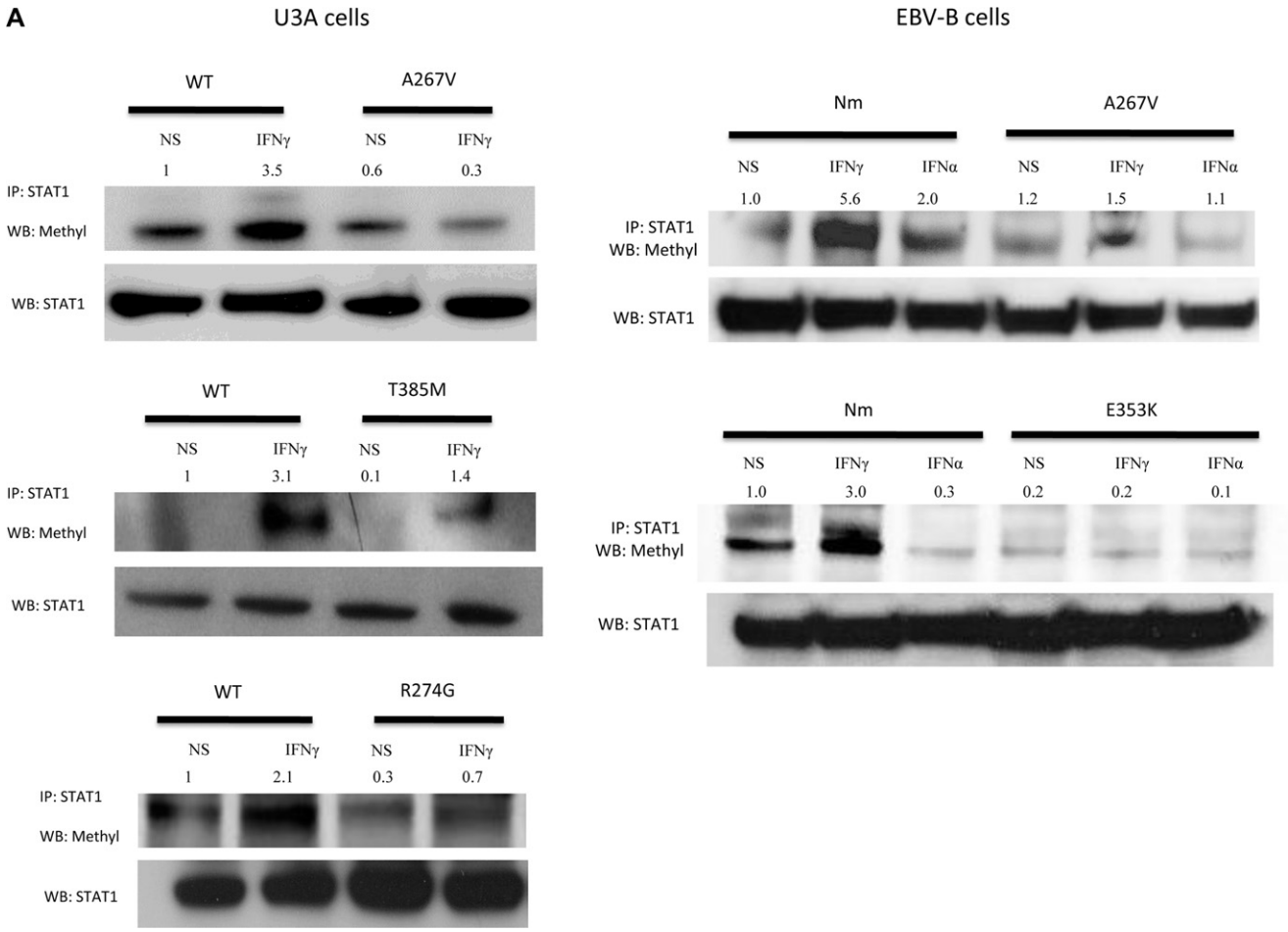

FIG E4. STAT1-associated methylation in patients' cells. **A,** Cell lysates were obtained from transfected U3A cells or EBV-B cells stimulated or not stimulated *(NS)* with IFN-γ or IFN-α (30 minutes). After immunoprecipitation with anti-STAT1 antibody, blots were developed with anti-DMA, stripped, and reprobed with anti-STAT1. Lower methyl-associated STAT1 expression was observed in mutant compared with normal cells. Blots are representative of 3 individual experiments. **B,** B cells from patients with mutations and normal B cells pretreated with SAMe were stimulated with IFN-γ and IP:WB anti-STAT1:anti-DMA, anti-PIAS1, and anti-STAT1. Blots are representative of 2 independent experiments. **C,** Treatment of B cells with SAMe decreased pSTAT1 expression in IFN-γ–stimulated cells. Blots are representative of 3 independent experiments for each condition. Numbers are band densities are normalized to the unstimulated samples. *NM*, Control subjects.

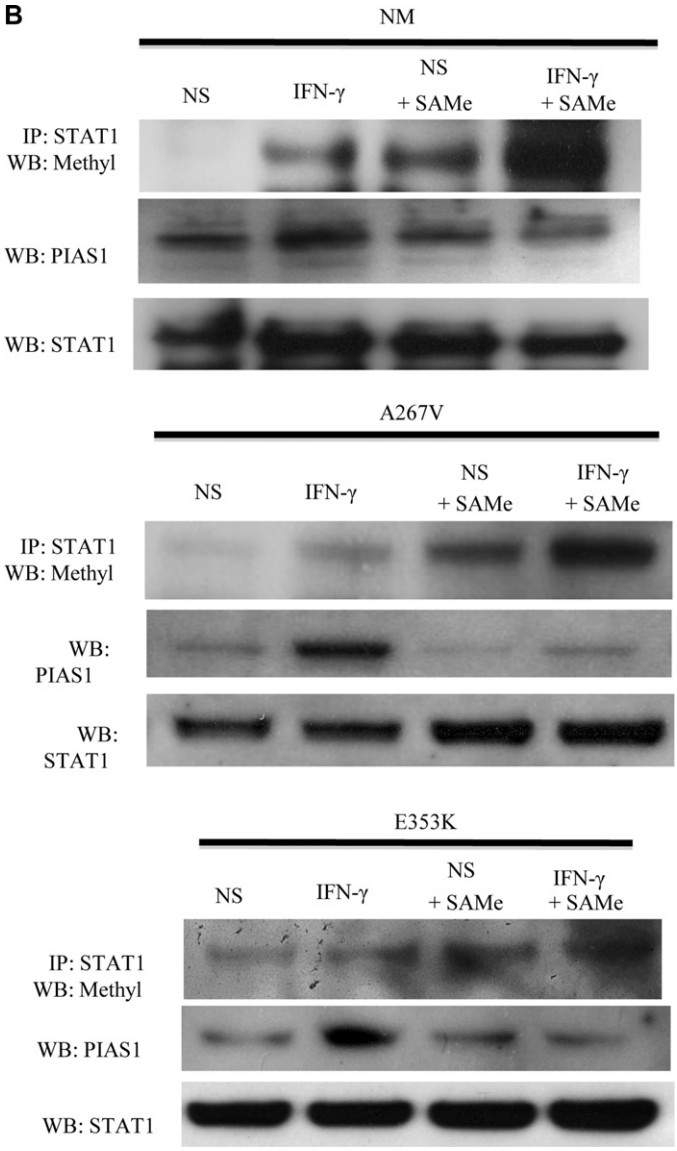

FIG E4. *(Continued)*

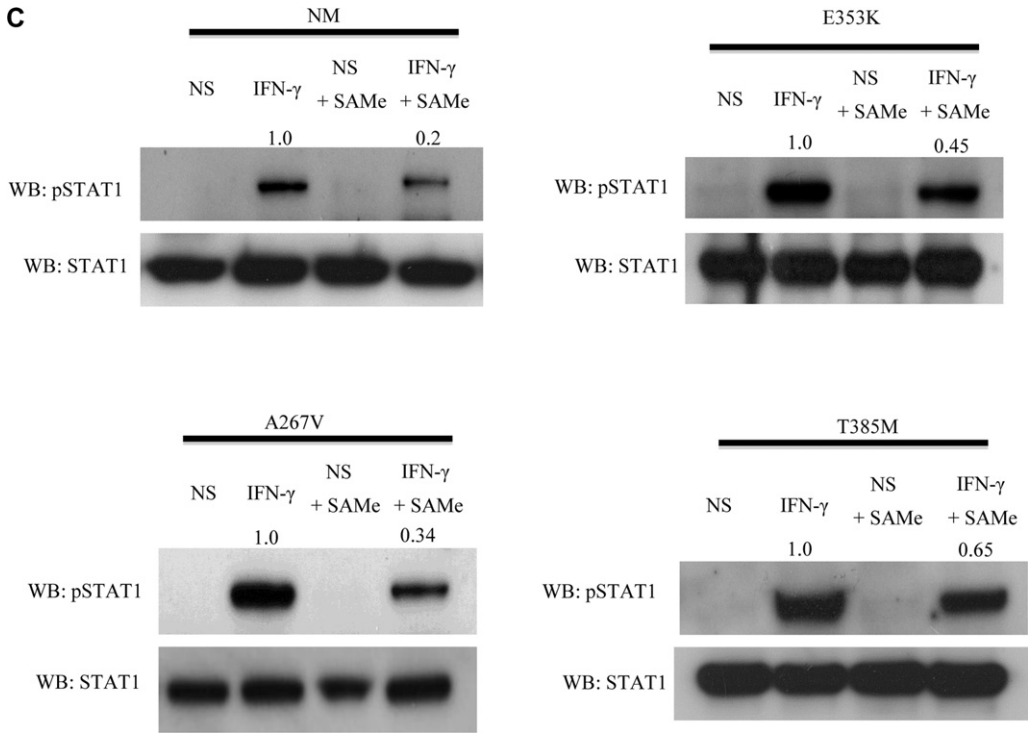

FIG E4. *(Continued)*

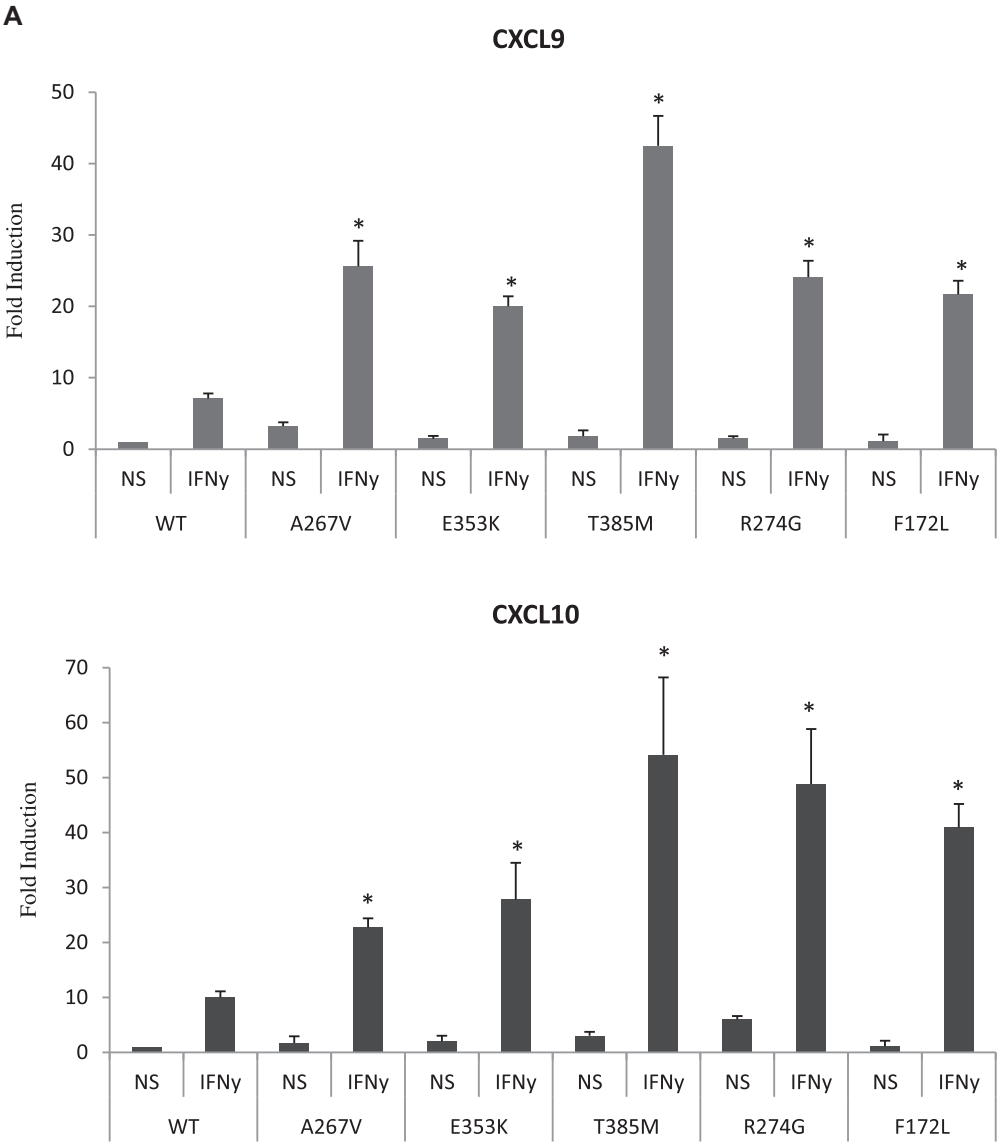

FIG E5. Expression of IFN-γ (*CXCL9* and *CXCL10*; **A**) and IFN-α (*MX1* and *ISG15*; **B**) target genes in U3A cells transfected with WT or patients' constructs stimulated with IFN-γ or IFN-α, respectively. **P* < .05 when compared with WT cells. **C,** Restimulation experiments performed in primary human PBMCs (patients and healthy donors). Results are means ± SDs of 3 independent experiments. *NS,* Nonstimulated; *Nm,* control subjects. **P* < .05 compared with IFN-γ rest.

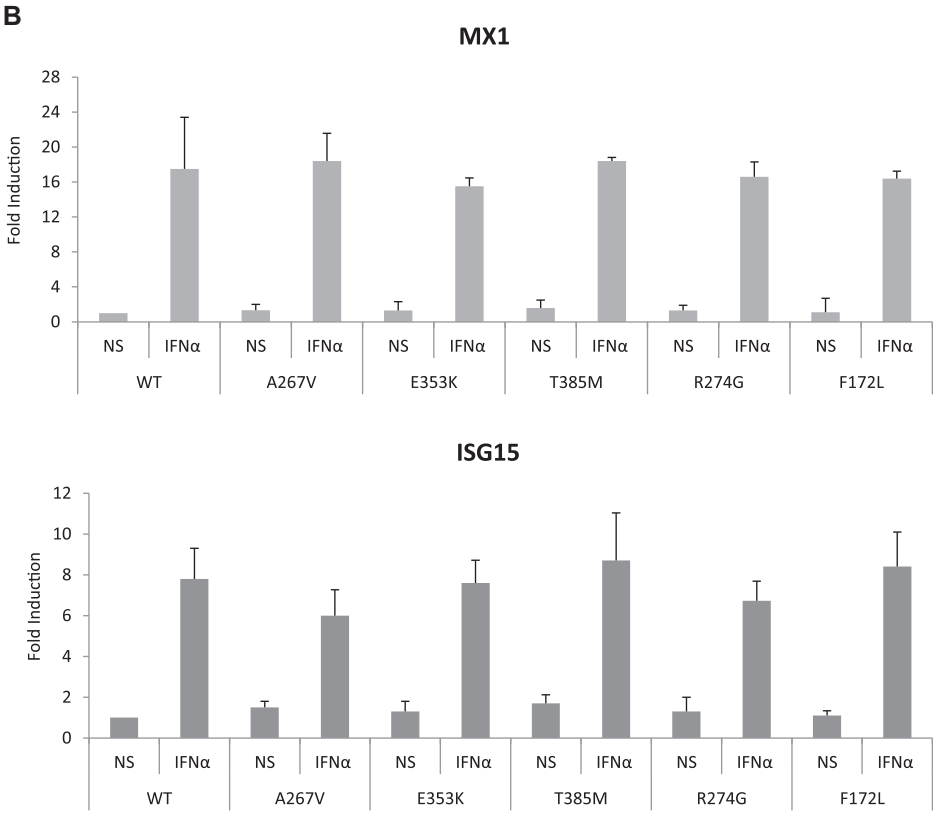

FIG E5. *(Continued)*

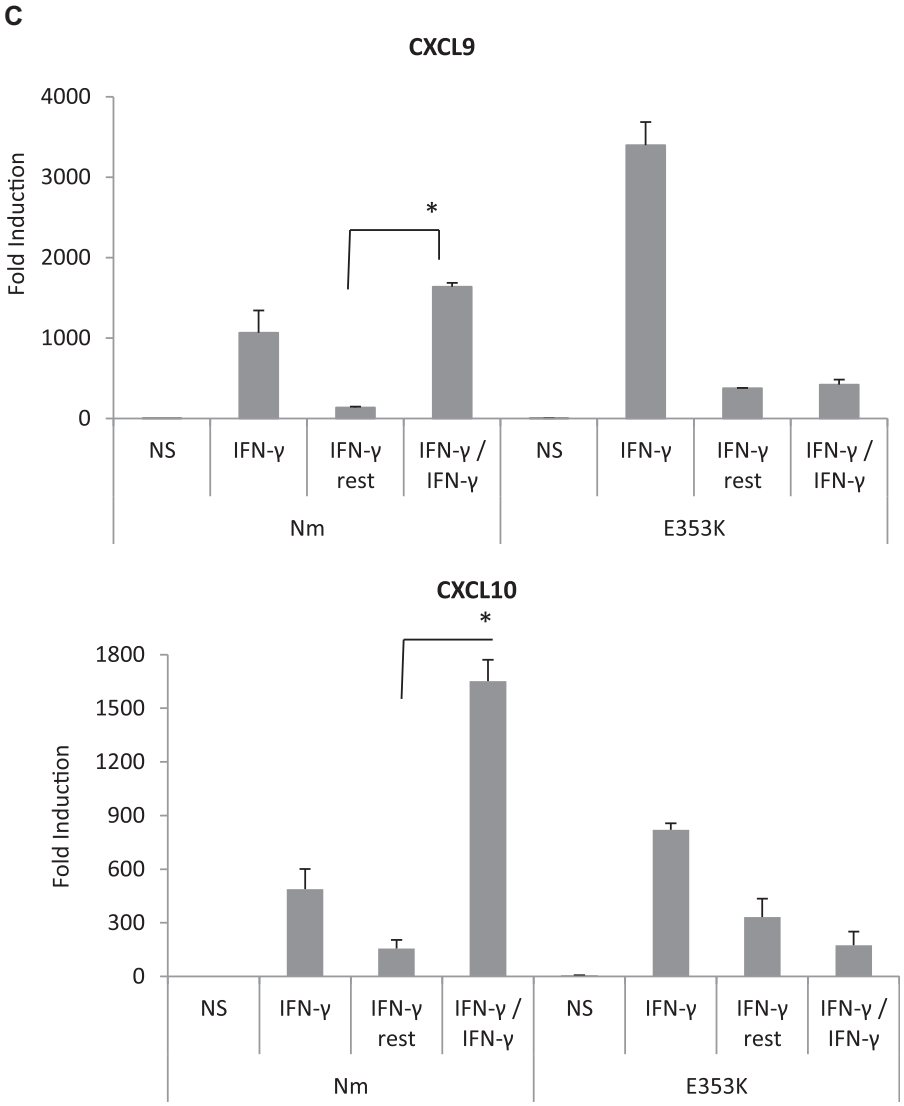

FIG E5. *(Continued)*

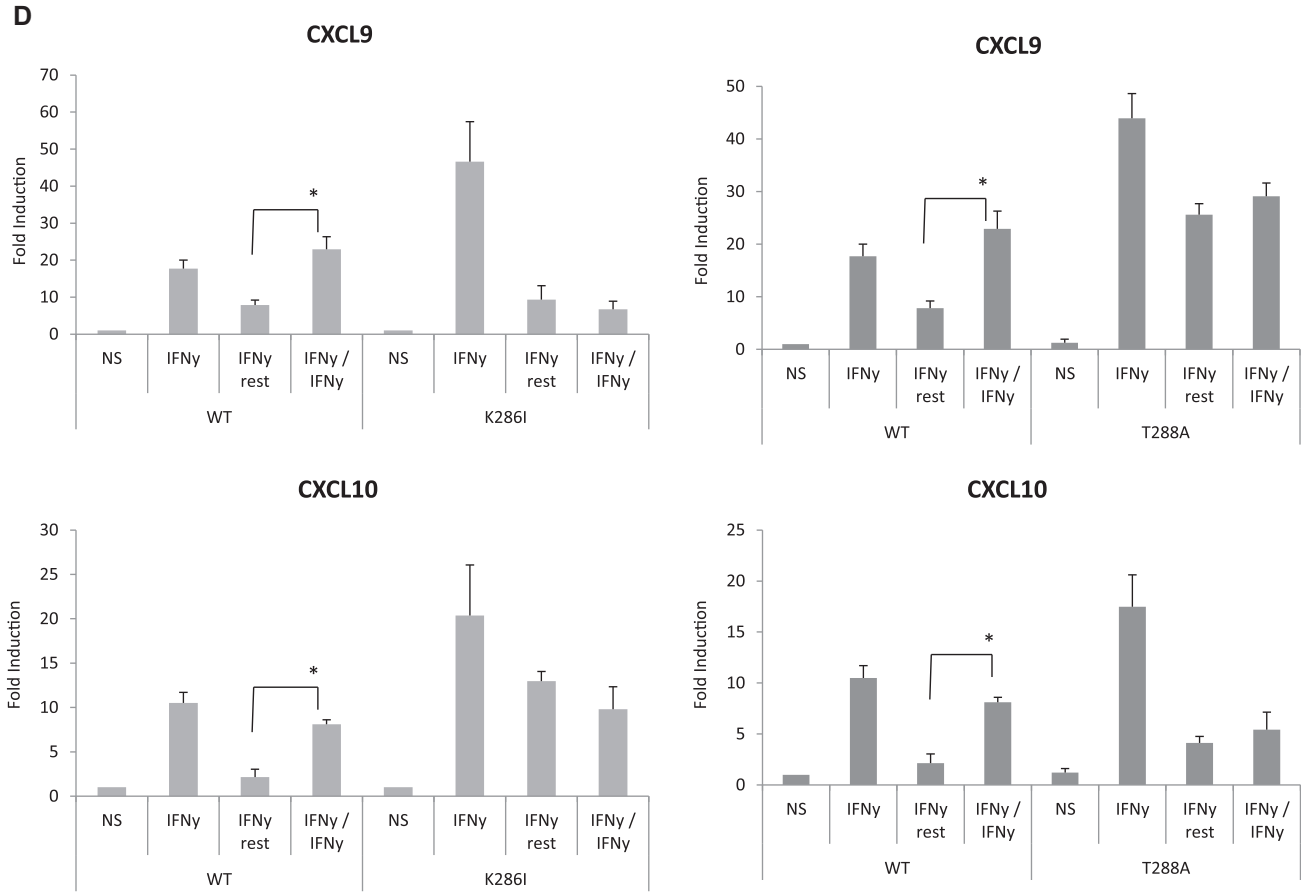

FIG E5. *(Continued)*

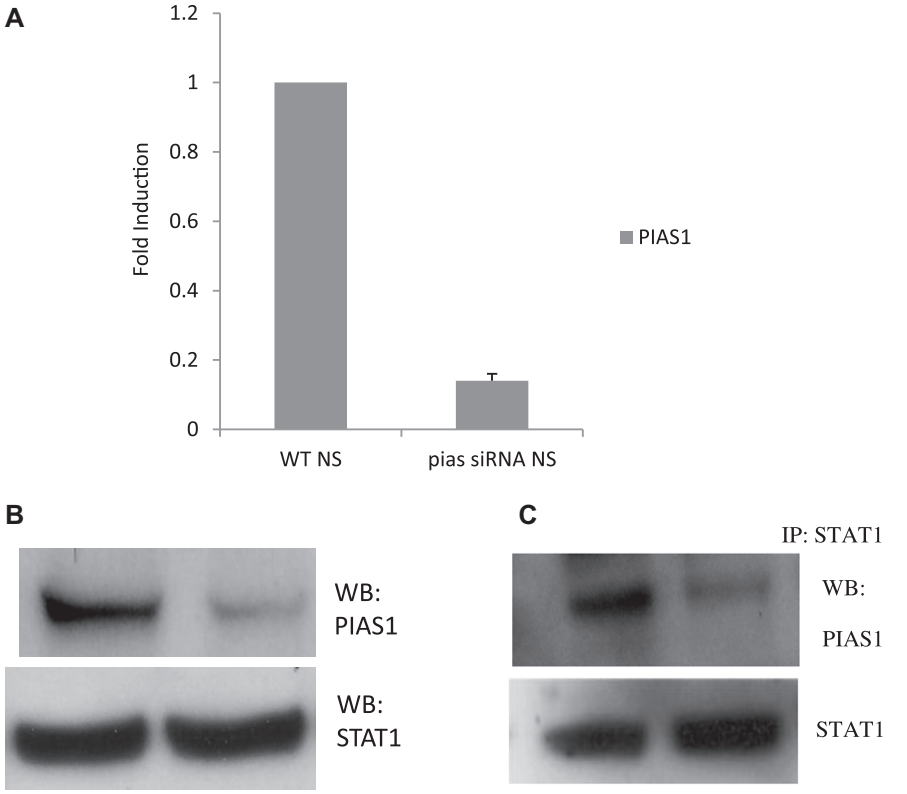

FIG E6. Knockdown of PIAS1. **A,** Levels of message for PIAS1 are diminished after knockdown by using siRNA PIAS1 in U3A cells. **B** and **C,** U3A cell lysates were blotted for PIAS1 (Fig E6, *B*) or IP:WB STA1:PIAS1 (Fig E6, *C*), showing lower PIAS1 association with STAT1. *NS,* Nonstimulated.

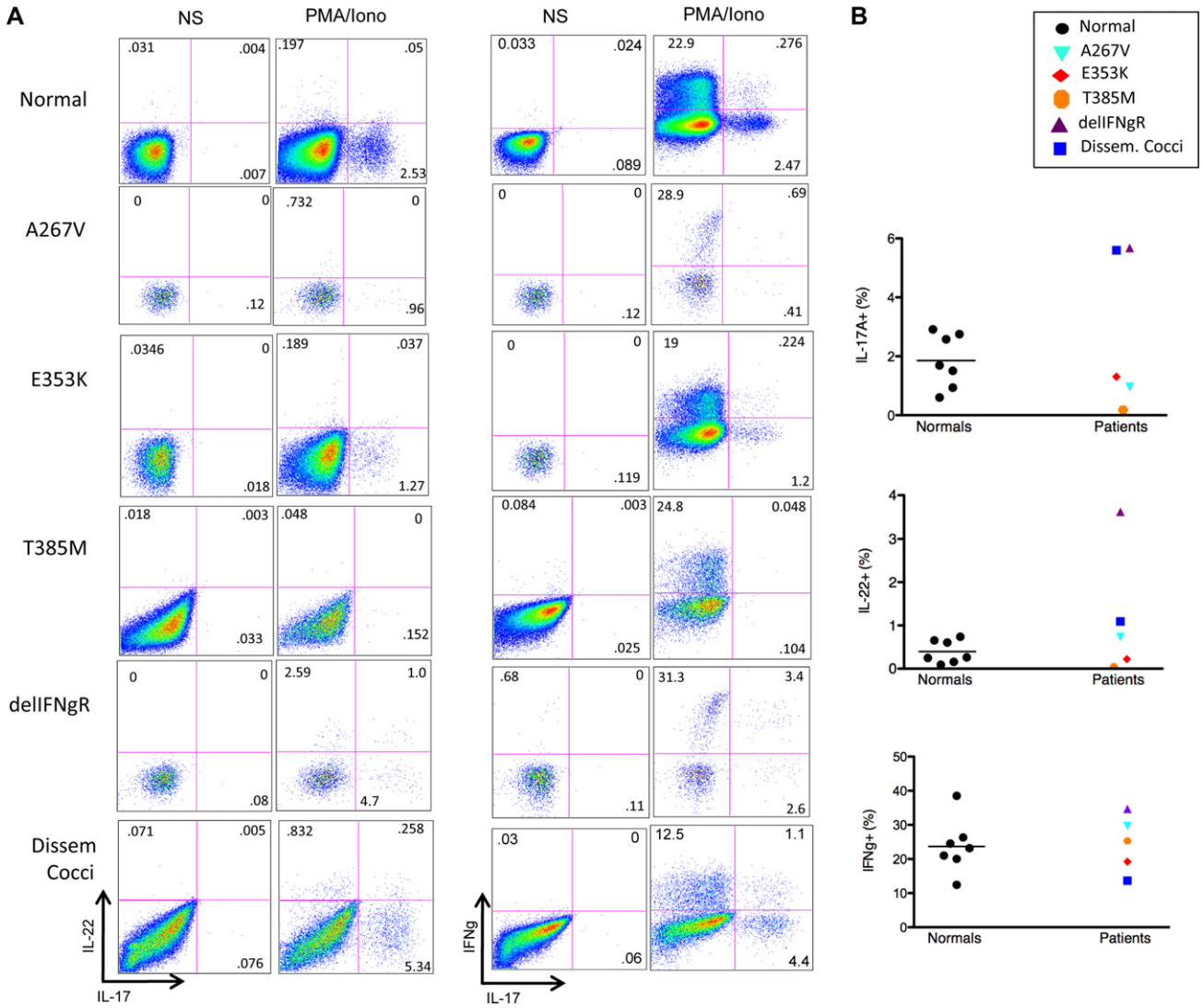

FIG E7. Evaluation of T_H17 function in PBMCs from healthy donors (n = 7), STAT1 mutants, a del*IFNGR1* patient, and 1 patient with disseminated coccidioidomycosis of unknown cause. **A,** *Dot plots* are representative of 2 to 4 experiments for each subject. **B,** Percentage of $CD3^+CD4^+CD45RO^+$ cells producing IL-17, IL-22, and IFN-γ in response to phorbol 12-myristate 13-acetate plus ionomycin. *Horizontal bars* are the mean of the response in the control group. *NS*, Nonstimulated.